SECOND QUARTER 2010
VOLUME 18, NO. 2

RIAC

The Reliability Information Analysis Center (RIAC) is a DoD Information Analysis Center sponsored by the Defense Technical Information Center

JOURNAL

OF THE RELIABILITY INFORMATION ANALYSIS CENTER

STRUCTURAL RELIABILITY PROGNOSIS AND HEALTH ASSESSMENT OF AIRFRAMES USING NON-DESTRUCTIVE INSPECTION

Masoud Rabiei, Center for Risk and Reliability, Department of Mechanical Engineering, University of Maryland
Mohammad Modarres, Center for Risk and Reliability, Department of Mechanical Engineering, University of Maryland
Paul Hoffman, NAVAIR 4.3.3 Structures Division, Reliability and Risk Assessment Team Lead

Abstract

This paper describes part of a multi-year effort in prognosis and health monitoring (PHM) at the University of Maryland, College Park. The objective of this PHM effort is to develop a Bayesian framework based on mechanistic failure models and non-destructive inspection data to estimate airframe reliability and risks, and to support fleet management of aging aircraft. The ultimate goal is to develop an integrated probabilistic framework for utilizing all available information to better predict (with less uncertainty) risks and structural health of the aircraft. Such information includes fatigue models and test data, health monitoring measurements and inspection field data. Despite significant achievements in the modeling of crack growth behavior using fracture mechanics, it is still of great interest to find practical techniques for monitoring the crack growth instances using non-destructive inspections and to integrate such inspection results with the fracture mechanics models. In the work presented in this paper, a probabilistic damage-tolerance model based on acoustic emission (AE) monitoring is proposed to enhance the reliability and risk prediction for structures subject to fatigue cracking.

Introduction

Authors have previously proposed a probabilistic model (Wang et al., 2009) to assess the reliability of aging airframes by predicting the probability that a fatigue-induced crack will reach a length that poses unacceptable risk after specified future flight hours. They have also shown (Wang et al., 2008) that using prediction models alone cannot assure the safety of a mission. The next step towards enhancing the quality of risk predictions is to use non-destructive inspection (NDI) to monitor the crack growth in the structure and to supplement the mechanistic fatigue model predictions by this extra information.

Over the past 30 years, acoustic emission technology has been developed as a promising and effective NDI technique capable of detecting, locating and monitoring fatigue cracks in a variety of composite and metal structures such as airframes (Boller, 2001). Acoustic emissions are elastic stress waves generated by a rapid release of energy from localized sources within a material under stress (Mix, 2005). Such emissions often originate from defect related sources such as permanent microscopic deformations within material and fatigue crack extension.

In this paper we propose a method to use AE monitoring, instead of complex procedures and calculations, to determine the stress intensity range ΔK in fatigue crack propagation. The value of ΔK depends on the geometry, stress amplitude and the instantaneous crack size. For a given geometry, a large ΔK represents either a large crack size and/or a high stress amplitude range applied to the structure. Stress intensity is a parameter that can be considered an aggregate driving force for fatigue crack growth. Fracture toughness K_{IC} on the other hand can be thought of as a measure of a material's resistance to stable crack propagation under cyclic loading (Anderson, 1994). The crack growth is stable as long as the stress intensity is less than the fracture toughness of the material.

To use AE monitoring for quantitative prognosis and health assessment, we define a risk factor based on the probability that the maximum stress intensity K_{max} estimated from AE signals, exceeds K_{IC} of the material.

In the following sections, first a brief overview of the experimental setup and procedure is given. Next, the correlation between AE signals and ΔK is established and a Bayesian regression approach is used to find the probability density function (PDF) of K_{max} and consequently calculate R_{AE} as a function of AE parameters.

Acoustic Emission Response During Fatigue Crack Growth

Several investigators have studied the connection between fatigue crack growth behavior and the resulting acoustic emissions (Hamel et al., 1981; Bassim et al., 1994). Certain features of acoustic emission signals are found to be stochastically correlated with key fatigue parameters such as ΔK and crack growth rate. For instance, AE counts c which is the number of times that the AE signal amplitude exceeds a certain threshold value, and its derivative, count rate dc/dN, are two of the most commonly used AE parameters in fatigue. (Bassim et al., 1994) have shown that the AE count rate and ΔK have a power relationship as follows:

$$\frac{dc}{dN} = B' \Delta K^{\alpha'} \quad (1)$$

where c denotes the AE count, ΔK is the stress intensity range and B' and α' are model parameters which mainly depend on material properties and environment, and should be estimated experimentally. Our goal is to estimate ΔK using AE observations; therefore we use the inverse of Eq. **(2)** as follows:

$$\Delta K = B\left(\frac{dc}{dN}\right)^{\alpha} \quad (2)$$

where $B = B'^{-1/\alpha'}$ and $\alpha = 1/\alpha'$. The linear form of Eq. (2) yields:

$$\ln \Delta K = \alpha \ln\left(\frac{dc}{dN}\right) + \beta \quad (3)$$

where $\beta = ln\ B$ and will be estimated along with parameter α using the experimental results.

The significance of Eq. (1) is that once the model parameters are determined, one can use this equation to estimate ΔK by monitoring the acoustic emissions and extracting the AE count rate from the observed signals.

In order to verify the relationship proposed in Eq. (1) and to estimate its parameters we carried out experiments in which fatigue crack growth in a metallic specimen was monitored while the generated acoustic emission signals were captured for further analysis. Material properties and some of the geometrical features (e.g. thickness of the specimen) were selected similar to those of the real airframe. The tests were carried out on standard compact tension (CT) specimen (ASTM E647-08, 2008) made of 7075-T6 aluminum alloy (W=2.5 inch, B=0.125 inch) using a 5 kip MTS machine. The specimen was first fatigue pre-cracked using sinusoidal loading with a min-max loading ratio R=0.1 and a frequency of 30 Hz until fatigue crack of adequate length and straightness in accordance with ASTM E647 was detected. The main fatigue test was performed at a frequency of 10 Hz using the same R ratio of 0.1. The applied load range was determined according to the material properties and geometry of the test specimen and remained fixed throughout the test. Macro digital photography was used for crack size measurement; high resolution pictures of the specimen (with a scribed scale attached to it) were automatically taken using time-lapse photography techniques. The pictures were post-processed using the Image Processing Toolbox in MATLAB to identify the crack tip. The crack length was then measured with an accuracy of 0.01 inch.

A PCI-2 AE monitoring system supplied by Physical Acoustic Corporations was used to capture the AE signals. A wideband (WB) sensor was clamped on the specimen with silicon grease used as a coupling agent. AE signals were first amplified using a 40 dB differential amplifier. A 200 kHz high pass filter was used to filter out the extraneous noise mostly from the MTS machine. Signals with amplitudes exceeding a threshold of 45 dB were transferred to a computer for feature extraction. Several AE features were calculated by the system and recorded for further analysis. Time domain features included hit time, counts, amplitude, duration, absolute energy and load level. Frequency domain features included peak frequency and frequency centroid (a measure of average frequency) of the signals. Fatigue crack growth data (applied load history, crack size a and number of elapsed cycles N) were recorded as well. Fatigue data and AE were synchronized on a single PC to facilitate further analysis.

continued on next page ›››

continued from page 3

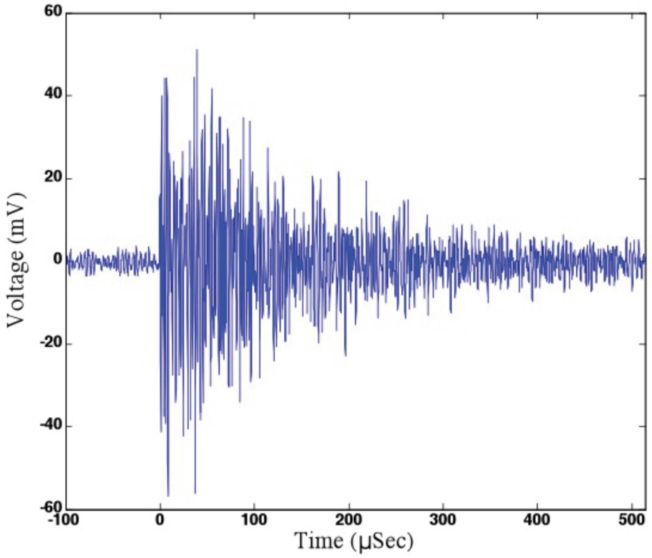

Figure 1: Typical AE signal due to crack growth

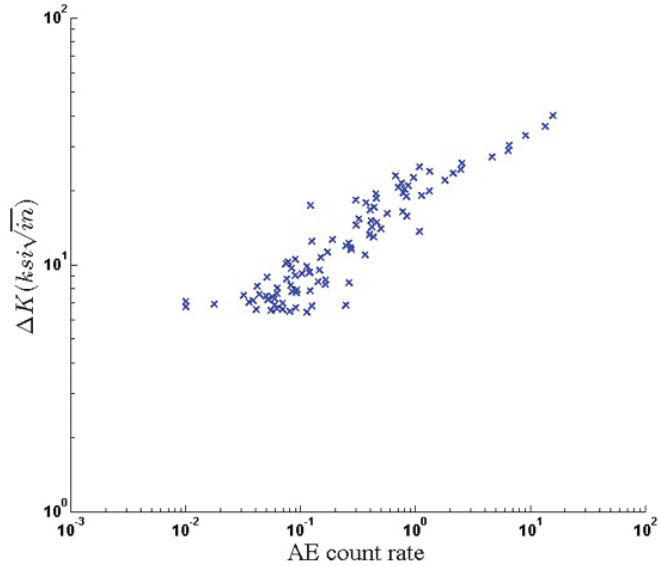

Figure 2: Correlation between AE count rate and ΔK after filtration

Figure 1 shows a typical AE signal generated during fatigue crack growth.

Signals received during AE testing are often buried in noise from numerous sources such as surface rubbing at loading pins, noise from the hydraulic loading actuators, internal rubbing of crack surfaces, etc. Researchers (Berkovits and Fang, 1995; Fang and Berkovits, 1993) have proposed different de-noising techniques to overcome this shortcoming.

The majority of investigators including the authors of this paper suspect that only events occurring near the maximum load in a cycle are associated directly with crack extension (Roberts and Talebzadeh, 2003). In the present study, we found that the events (i.e., AE hits) occurring within the top 30% of the peak load have a good correlation with ΔK and consequently the crack growth rate. The second criterion used for AE filtration was that the events occurring during the loading portion of a cycle are more likely to be due to crack extension versus those occurring during the unloading part. Figure 2 shows the log-linear correlation between ΔK and the AE count rate, once proper filtration is performed so that the AE signals generated from crack extension are separated from the noise. This result is in good agreement with the linear model proposed in Eq. (3).

Figure 3 shows the AE count rate and the crack growth rate on the same plot. It is notable how both rates increase with a similar slope when plotted on a log-log scale against ΔK. This suggests that by monitoring the AE count rate, one can describe the crack growth behavior without directly measuring the actual crack size or its rate of growth.

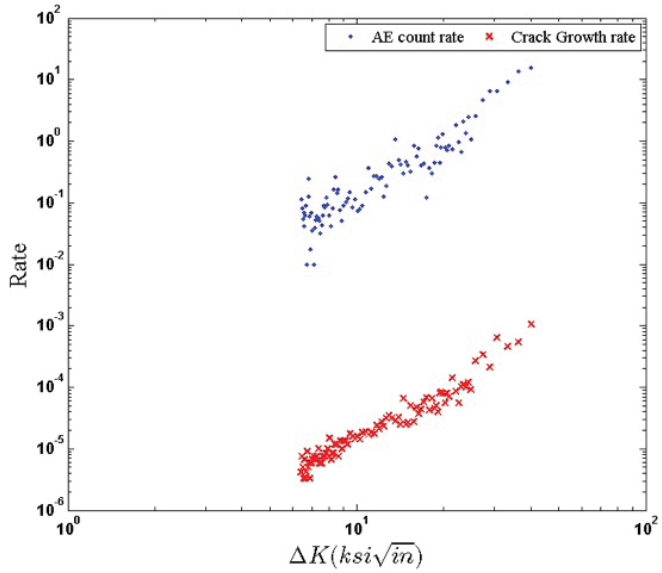

Figure 3: Strong linear correlation between the stress intensity range and both AE count rate and crack growth rate

Bayesian Parameter Estimation

In this section, a Bayesian regression technique is used to estimate the parameters α and β of Eq. (3) including their uncertainties. Rather than relying solely on the best estimate of the parameters and the corresponding confidence intervals, as is the common practice when using maximum likelihood estimation (MLE) and traditional regression techniques, Bayesian estimation provides a reasonable coverage of the uncertainties by calculating the joint PDF of the model parameters (See Figure 4). Another advantage of the Bayesian approach is that it preserves the available information in the scatter of the data in the form of posterior probability distributions for the model parameters.

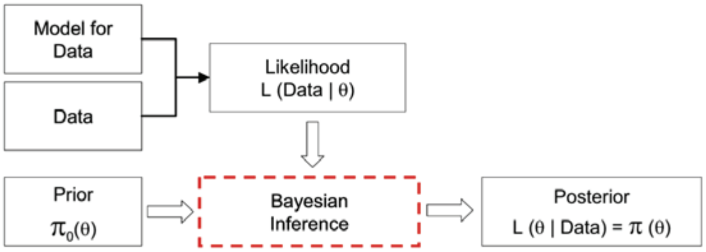

Figure 4: Bayesian Inference Framework (Azarkhail and Modarres, 2007)

In addition, the Bayesian inference technique provides a framework for incorporating additional sources of knowledge that may be available about the parameters. Possible sources of such information include similar past experiments, handbook data and expert judgment. See (Azarkhail and Modarres, 2007) for more information on using the Bayesian regression technique for uncertainty characterization.

In the Bayesian approach to regression, the fitness concept is represented in the probability of occurrence or likelihood form where a larger value of the likelihood function shows a better model fit to the data. An alternative way to define the likelihood function is to use the distribution of "model error". Here error is defined as the difference between the model prediction and the observed data and can be treated as a random variable. It is assumed that for the best fitted model, the error is normally distributed with mean zero and unknown standard deviation s. This is equivalent to assuming that the dependent variable is normally distributed with its mean defined by the model prediction and with standard deviation s. Here we define the likelihood function by assuming that the dependent variable in DK is normally distributed according to Eq. (4).

$$\ln \Delta K \sim \mathrm{N}(\mu,\sigma) \quad (4)$$

where $\mu = \beta + \alpha \ln(dc/dN)$ is the mean of the normal PDF, which is calculated based on the linear relationship in Eq. (3). Also, σ is the standard deviation, which is an unknown parameter to be estimated along with α and β. The conditional likelihood function can then be formally defined as follows:

$$L\left(\ln \Delta K, \ln\left(\frac{dc}{dN}\right) \middle| \alpha,\beta,\sigma\right) = \prod_{i=1}^{n} \frac{1}{\sqrt{2\pi}\sigma} e^{-\frac{1}{2}\left(\frac{\ln \Delta K_i - \beta - \alpha \ln\left(\frac{dc}{dN}\right)_i}{\sigma}\right)^2} \quad (5)$$

Bayesian inference starts with an uncertain and subjective belief about the model parameters. This belief is systematically updated using the likelihood function (Eq. (5)) and in light of the available data (i.e. ordered pairs of ($\ln \Delta K_i$, $\ln (dc/dN)_i$). In this study, we started with no past experience, and therefore no prior information about the distribution of parameters was available. This is reflected in our choice of non-informative (uniform) prior distributions for parameters α, β and σ. If additional information such as similar test results or prior estimates of the model parameters becomes available, an informative prior distribution can be used instead. This will affect the posterior distribution of parameters accordingly. Notice that when uniform priors are used for the parameters, the Bayesian and MLE approach will both result in the same best estimate for the parameters but the coverage of the uncertainty over the parameters could be different. Uncertainty bounds in MLE are estimated using a Fisher information matrix with an underlying normality assumption for the parameters whereas in the Bayesian approach, the uncertainty bounds are derived using the posterior joint distribution of parameters. Figures 5 and 6 show the Bayesian regression results in the form of the marginal and joint posterior distribution of model parameters, respectively.

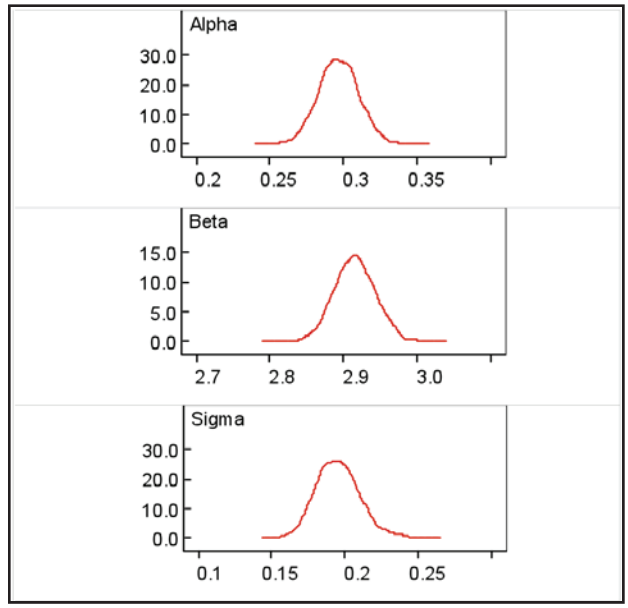

Figure 5: Marginal posterior PDF of model parameters

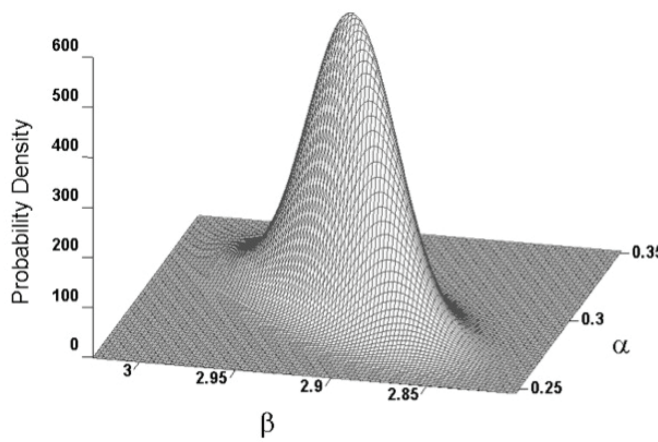

Figure 6: Posterior joint PDF of α and β

In a Bayesian framework, prediction at a given value of the independent variable is based on the predictive distribution, that is, the likelihood of the future data averaged over the posterior distribution of parameters as illustrated in Eq. (6).

$$f\left(\Delta K \mid \frac{dc}{dN}\right) = \iiint_{\underline{\theta}} f\left(\Delta K \mid \frac{dc}{dN}, \underline{\theta}\right)\pi(\underline{\theta})\, d\underline{\theta} \quad (6)$$

where $\pi(\underline{\theta})$ represents the posterior distribution and $\underline{\theta} = \{\alpha,\beta,\sigma\}$ is the vector of model parameters.

continued on next page ›››

continued from page 5

For complex likelihood functions with a large number of parameters it may be very difficult and sometimes impossible to solve these equations analytically. Therefore, in practice, numerical approaches such as Monte Carlo based methods are used to calculate these multidimensional integrals. In this approach, the characteristics of distributions are estimated by generating a sufficient number of statistical samples from them. Here we use samples from the posterior joint distribution of model parameters along with Eq. (3) to estimate the distribution of ΔK for a given value of dc/dN. Once ΔK is estimated, the maximum stress intensity $K_{max} = \Delta K/(1-R)$ can be easily calculated for a given loading ratio R.

Probabilistic Reliability Model

As the final step to develop an AE-based prognosis and health monitoring approach, we define an instantaneous risk factor R_{AE} based on the conditional distribution of K_{max} and the value of fracture toughness K_{IC}. R_{AE} is defined in Eq. (7) as the probability that the maximum stress intensity exceeds the fracture toughness of the material that results in unstable crack growth and ultimately failure.

$$R_{AE} = \Pr(K_{max} > K_{IC}) = 1 - F_{K_{max}}(K_{IC}) \quad (7)$$

where $F_{K_{max}}$ is the Cumulative Density Function (CDF) of K_{max}.

R_{AE} could also be thought of as the probability of transitioning from stage II to stage III of fatigue crack growth regime. This transition probability is calculated at any given point in time, based on the AE inspection results.

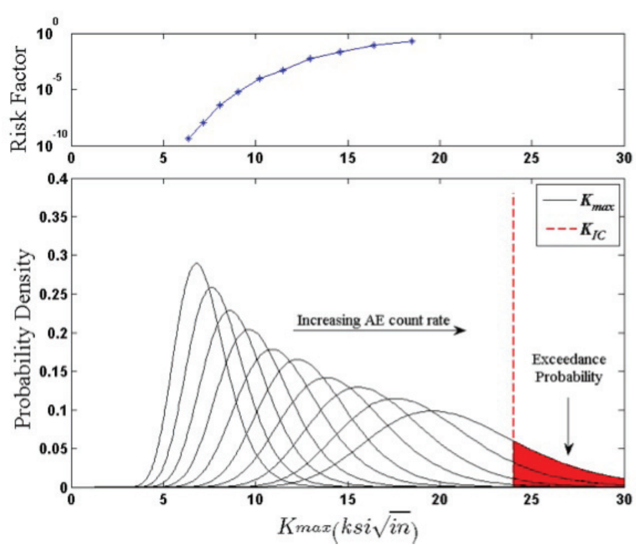

Figure 7: PDF of K_{max} as the AE count rate increases (bottom), Increasing trend in risk factor (top)

Figure 7 shows the conditional PDF of K_{max}, estimated from the AE data in Figure 2. Notice how this distribution shifts to the right as the AE count rate increases. This figure also illustrates the increasing trend in R_{AE} as the AE count rate and K_{max} increase throughout the experiment. By monitoring the acoustic emissions from a structure, the proposed approach enables us to estimate, at a given point in time, the probability that the crack growth transitions to the unstable regime and ultimately leads to failure.

Here a deterministic K_{IC} value is assumed for simplicity but if additional data about the statistical distribution of K_{IC} becomes available, the methodology presented here can be used to calculate the risk factor accordingly.

Once the transition probability is calculated, a decision-maker will be able to compare it with a threshold value set according to the tolerable risk in the system and use this information as a guideline for assessing the structural safety of the aircraft.

Summary

A damage-tolerance reliability model for structural health monitoring was presented in this paper. Experiments were carried out to use AE inspection to estimate the stress intensity range ΔK during fatigue crack propagation in a standard CT specimen. Acoustic emission signals were properly filtered and features relevant to fatigue crack growth were extracted. The linear model proposed in the literature for $\ln(\Delta K)$ versus $\ln(dc/dN)$ was confirmed using experimental data. Bayesian regression was used to estimate the marginal and joint probability distributions of the model parameters. Next, the conditional PDF of ΔK given the AE count rate was calculated. Finally, a risk factor R_{AE} was defined based on the probability that K_{max} exceeds the fracture toughness of the material K_{IC} given the AE inspection results. There is room for several improvements in this study. The approach proposed here is also applicable to the case of random amplitude loading when revised to account for the variability in the applied loading. Also, AE filtration and feature extraction can be done in a more sophisticated manner by wavelet analysis and by taking into account more time and frequency domain AE parameters.

Acknowledgment

This work was supported by a grant from the Naval Air Systems Command (NAVAIR) under a cooperative agreement between the University of Maryland and NAVAIR. The authors would like to express thanks to Dr. Hugh Bruck of the University of Maryland and Dr. Valery Godinez of Physical Acoustics Corp. for their help in setting up the acoustic emission experiments.

Nomenclature

ΔK	stress intensity range
K_{max}	maximum stress intensity
K_{IC}	fracture toughness
dc/dN	acoustic emission count rate
R_{AE}	risk factor based on acoustic emission
α, β, σ	model parameters

References

1. (Anderson, 1994) Anderson, T. L. *Fracture Mechanics: Fundamentals and Applications, Second Edition*. 2nd ed. CRC, December 16, 1994.

2. (ASTM E647-08, 2008) ASTM E647-08. *Standard Test Method for Measurement of Fatigue Crack Growth Rates*. ASTM International, 2008.

3. (Azarkhail and Modarres, 2007) Azarkhail, M., and M. Modarres. A Novel Bayesian Framework for Uncertainty Management in Physics-Based Reliability Models. In *ASME International Mechanical Engineering Congress and Exposition*. Seattle, Washington, USA, November 11, 2007.

4. (Bassim *et al.*, 1994) Bassim, M. N., S. St Lawrence, and C. D. Liu. Detection of the onset of fatigue crack growth in rail steels using acoustic emission. *Engineering Fracture Mechanics* 47, no. 2: 207-214, 1994.

5. (Berkovits and Fang, 1995) Berkovits, Avraham, and Daining Fang. Study of fatigue crack characteristics by acoustic emission. *Engineering Fracture Mechanics* 51, no. 3 (June): 401-409, 1995.

6. (Boller, 2001) Boller, C. Ways and options for aircraft structural health management. *Smart materials and structures* 10, no. 3: 432-440, 2001.

7. (Fang and Berkovits, 1993) Fang, D., and A. Berkovits. Fatigue damage mechanisms on the basis of acoustic emission measurements. In *Novel experimental techniques in fracture mechanics: presented at the 1993 ASME Winter Annual Meeting New Orleans, Louisiana November 28-December 3, 1993*, 219. American Society of Mechanical Engineers, 1993.

8. (Hamel *et al.*, 1981) Hamel, F., J. P. Bailon, and M. N. Bassim. Acoustic emission mechanisms during high-cycle fatigue. *Engineering Fracture Mechanics* 14, no. 4: 853-860, 1981.

9. (Mix, 2005) Mix, P. E. *Introduction to nondestructive testing: a training guide*. Wiley-Interscience, 2005.

10. (Roberts and Talebzadeh, 2003) Roberts, T. M., and M. Talebzadeh. Acoustic emission monitoring of fatigue crack propagation. Journal of Constructional Steel Research 59, no. 6 (June): 695-712, 2003.

11. (Wang et al., 2008) Wang, X., M. Rabiei, M. Modarres, and P. Hoffman. A probability-based individual aircraft tracking approach for airframe integrity. In Aging Aircraft 2008. Phoenix AZ, April, 2008.

12. (Wang *et al.*, 2009) Wang, X., M. Rabiei, J. Hurtado, M. Modarres, and P. Hoffman. A probabilistic-based airframe integrity management model. *Reliability Engineering & System Safety* 94, no. 5 (May): 932-941, 2009.

JUNE

S	M	T	W	T	F	S
		1	2	3	4	5
6	7	8	9	10	11	12
13	14	15	16	17	18	19
20	21	22	23	24	25	26
27	28	29	30			

RIAC Open Training Program //Virginia Beach, VA

June 8-10, 2010 and June 15-17, 2010
Contact: Pat Smalley, Reliability Information Analysis Center // P 877.363.7422 or 315.351.4200 // F 315.351.4209 // psmalley@theRIAC.org

International Applied Reliability Symposium // Reno, NV

June 15, 2010 thru June 17, 2010
Contact: P 888.886.0410 (toll free) or 520.886.0410 // Info@ARSymposium.org

JULY

S	M	T	W	T	F	S
				1	2	3
4	5	6	7	8	9	10
11	12	13	14	15	16	17
18	19	20	21	22	23	24
25	26	27	28	29	30	31

20th Anniversary INCOSE International Symposium // Chicago, IL

July 12, 2010 thru July 15, 2010
Contact: www.incose.org/symp2010/

3rd International Conference on Applied Human Factors and Ergonomics // Miami, FL

July 17, 2010 thru July 20, 2010
Contact: Gavriel Salvendy // salvendy@purdue.edu

2010 Annual ITEA Technology Review // Charleston, SC

July 20, 2010 thru July 22, 2010
Contact: www.itea.org/2010_Tech_Review_ws.asp

Performance Based Logistics - PBL 2010 // Arlington, VA

July 26, 2010 thru July 28, 2010
Contact: P 888.482.6012 // F 646.200.7535 // PBL@wbresearch.com

AUGUST

S	M	T	W	T	F	S
1	2	3	4	5	6	7
8	9	10	11	12	13	14
15	16	17	18	19	20	21
22	23	24	25	26	27	38
29	30	31				

10th International Conference on Cognitive Modeling // Philadelphia, PA

August 5, 2010 thru August 8, 2010
Contact: iccm2010@cs.drexel.edu

45th Annual International Logistics Conference and Exhibition // Dallas, TX

August 15, 2010 thru August 19, 2010
Contact: SOLE - The International Society of Logistics // P 301.459.8446 // F 301.459.1522 // solehq@erols.com

28th International System Safety Conference // Minneapolis, MN

August 30, 2010 thru September 3 2010
Contact: David Sullivan-Nightengale // P 651.489.1225 // sulli91a@my.erau.edu

SEPTEMBER

S	M	T	W	T	F	S
			1	2	3	4
5	6	7	8	9	10	11
12	13	14	15	16	17	18
19	20	21	22	23	24	25
26	27	28	29	30		

2010 Annual ITEA Conference // Glendale, AZ

September 13, 2010 thru September 16, 2010
Contact: www.itea.org/Annual_Symposium.asp // P 703.-631.6220 // F 703.631.6221

RIAC Open Training Program // Bellevue, WA

September 14,2010 thru September 16, 2010
Contact pat Smalley, Reliability Information Analysis Center // P 877.363.7422 or 315.351.4200 // F 315.351.4209 // psmalley@theRIAC.org

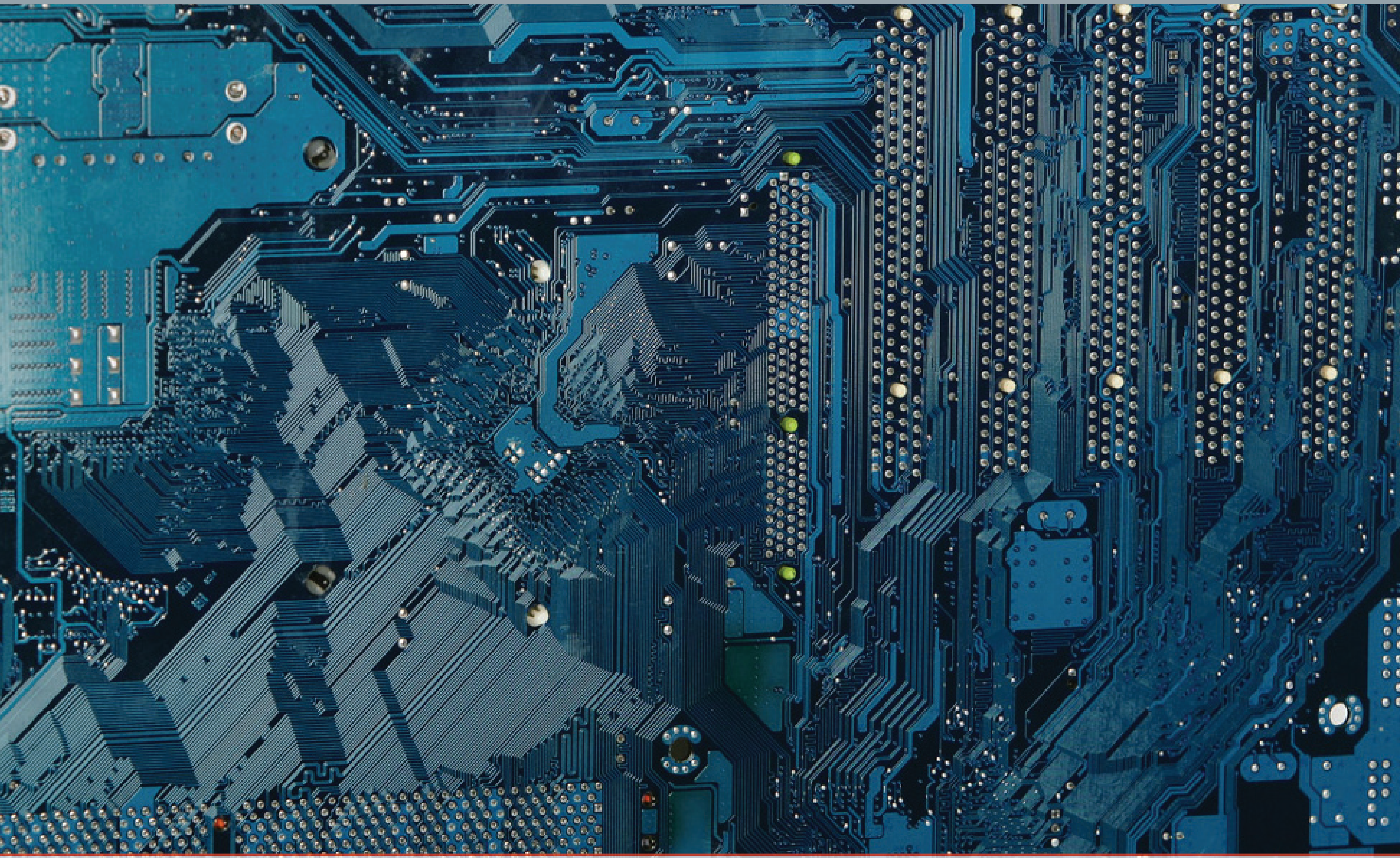

USING AVAILABILITY ANALYSIS TO REDUCE TOTAL COST OF OWNERSHIP

Bill Lycette, Agilent Technologies

Total Cost of Ownership (TCO) gained popularity with electronics manufacturers in the early 1990's when many industries, especially semiconductor equipment users, wanted to recognize that the procurement decision encompassed much more than the initial acquisition (purchase) cost. Indeed, if you consider costs associated with owning and operating the asset over its entire useful life, it is common for operational costs to considerably exceed acquisition costs.

This article introduces a TCO model that has been developed by Agilent Technologies. A key component of the TCO model is the notion of downtime mitigation. By way of example, the article shows how availability analysis can be used to improve system uptime and reduce the cost to own and operate the equipment.

Total Cost of Ownership Modeling

TCO is defined to be the total cost to own and operate a piece of equipment over its useful life. Agilent Technologies has developed a TCO model comprised of the two core elements of capital expenses (acquisition costs) and operating expenses that describe these costs at a high level. Modeling of capital expenses is fairly straightforward with depreciation schedules being the principle area of variation. Capital expenses generally are costs (C_{acq}) incurred to acquire and install the equipment. Operating expenses provide an area for much greater latitude in terms of what is included in the TCO model and how the cost components are represented. The TCO model presented in this article structures operating expenses in the following manner:

- Preventive Maintenance – C_{pm}
- Corrective Maintenance – C_{cm}
- Downtime Mitigation – C_{dm}
- Technology Refresh – C_{tr}
- Training & Education – C_{te}
- Resale value or disposal cost – C_{rv}
- Other – C_o

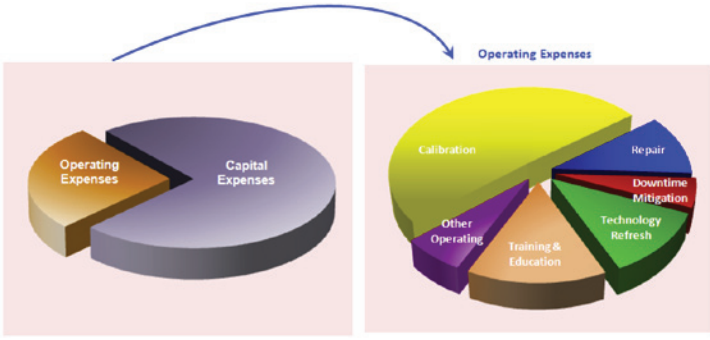

Figure 1. Capital Expenses and Operating Expenses represented in the TCO model.

The Total Cost of Ownership equation is given by:

$$TCO = C_{acq} + C_{pm} + C_{cm} + C_{dm} + C_{tr} + C_{te\,+}\, C_{rv} + C_{o}$$

Agilent Technologies is a leader in the electronic Test & Measurement industry. Typically calibration of the equipment is the single largest cost component of preventive maintenance expenses. In this regard, calibration cycle period is the single largest lever to pull on to reduce such metrology costs. Other important variables beyond just the cost to perform a calibration include cal turnaround time (TAT), logistical costs and any "repair" costs required to adjust the product back into calibration. Preventive maintenance costs would also include other periodically scheduled actions such as proactive replacement of subassemblies that tend to exhibit wear out phenomena.

Corrective maintenance generally refers to unplanned downing events such as equipment failure. For the purposes of this TCO model, corrective maintenance costs are represented by the cost to perform the repair, re-calibrate after the repair, logistics to remove, ship and re-install, and performance verification of the equipment. The cost to perform the repair can be represented by either a contracted repair agreement or, if the owner wishes, to "self-insure" on a Per Incident (P.I.) basis. Annual P.I. repair expenses are modeled as the expected annual value calculated by multiplying the P.I. cost times the probability of failure occurring in a one year period. While at first glance it may appear that a P.I. strategy is the lower cost option, one must also consider that a repair contract usually results in a lower repair TAT and therefore lower downtime. A downtime cost penalty must be applied to recognize the fact that the equipment was unavailable for use by the owner. This is accomplished by applying a cost driver variable, such as a weekly rental rate proxy, to the cost equation such that:

Cost of Unavailability = (purchase price) x (rental rate proxy) x (repair TAT)

Weekly rental rates for performance measurement equipment typically run in the range of 2-5% of the purchase price.

The consequences of unplanned corrective maintenance events such as equipment failure can be extremely costly, even disastrous, for the enterprise. For instance, if a test system goes down in a volume manufacturing environment or in a critical R&D application, the impact can be lost sales and missed business opportunities that may cost the enterprise millions of dollars. Because of difficulties in quantifying and predicting the outcome of such events, the TCO model does not place this aspect of the cost element under the heading of corrective maintenance. Instead, these sort of "catastrophic" costs are addressed through cost avoidance measures and strategies described in the Downtime Mitigation section that follows later in this article.

Technology Refresh (sometimes termed Product Migration) refers to situations where equipment owners wish to upgrade their assets to products with increased levels of measurement capability or increased levels of measurement speed. Typically the largest component of product migration costs is the investment required by equipment owners to ensure backward/forward compatibility of the new piece of equipment in their test process. Costs associated with developing/editing test code to ensure compatibility in the test process can be quite high. These are one-time expenses that should be amortized over the installed base of equipment that derive the benefit.

At the end of the equipment's useful life, the asset is disposed of either by selling, trading in for credit, or having the equipment recycled. The first two options are treated as a negative cost in the TCO model. High resale value becomes a strategic advantage for suppliers of superior quality products when one looks at the TCO algorithm.

Other TCO costs that a business may wish to incorporate into the calculation include energy, floor space and consumable materials.

Next, we turn our attention to a critical TCO component the author refers to as Downtime Mitigation. This is an area in which reliability and quality professionals play a crucial role.

Downtime Mitigation

As mentioned earlier, unplanned downing events (failures) are probabilistic in nature with the potential for catastrophically high costs to the business. This makes it difficult to attach a cost estimate that is both accurate and believable. A better approach is to develop and implement operational strategies that mitigate (or eliminate) the effects of unplanned downing events. Engineering and management have a number of downtime mitigation strategies to select from, including:

1) High Reliability
   - Select a product that offers leading edge reliability.
2) Low Repair TAT
   - Select a return-to-depot service provider that offers lowest possible repair TAT.
   - Perform on-site repair, either by contracting with a service provider or by developing the capability internally.
   - Purchase extended warranty service contracts to reduce or eliminate logistical, administrative and procurement delays.

continued on next page ›››

 continued from page 11

3) Capacity
- Purchase extra manufacturing test capacity and hold in reserve.
- Purchase spare equipment.
- For self-maintainers, purchase spare parts.

The approach suggested in this article is to develop and implement a downtime mitigation strategy that enables the business to deliver on its commitments to customers while minimizing TCO. One way to evaluate these strategies is to conduct Availability analyses and select the option that strikes an optimum balance between maximizing system Availability (i.e. minimizing downtime), minimizing costs to implement the strategy, and minimizing ongoing operating costs.

Some factors at work in the TCO algorithm cause costs to vary over time. Reliability characteristics of equipment (influencing repair costs and downtime costs) and calibration cycle period (influencing metrology costs) are examples of two such factors. In order for businesses to properly plan for future operating costs, it is important that TCO costs be modeled over time (see Figure 2).

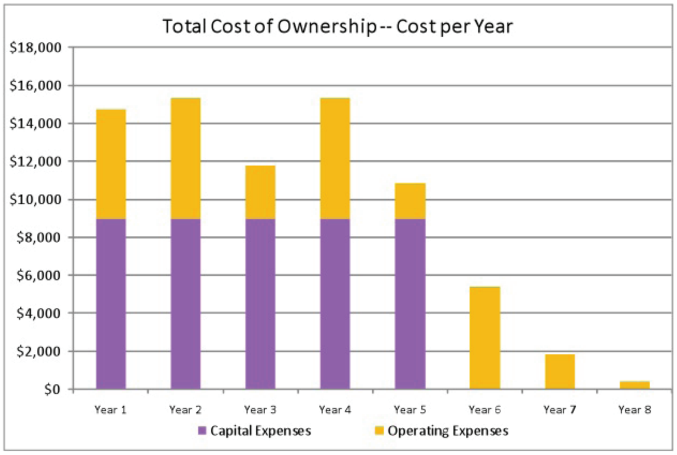

Figure 2. Total Cost of Ownership over time.

The example discussed later in this article illustrates the impact of these factors on a business' gross margins.

Availability

Availability is defined to be the probability that a given piece of equipment or system meets its intended function at a specified point in time. Factors that influence the Availability equation include the equipment's hazard function (instantaneous failure rate), repair TAT distribution, calibration TAT distribution and customer use model. Using specialized software and knowledge of product reliability and maintainability (R&M), we can model complex systems to arrive at a deep understanding of the variables that drive Availability of the "system."

Availability analysis at the system and subsystem levels provides clarity on the key drivers that most impact Uptime and TCO, thus enabling the business to make process recommendations for improving performance of the test system. From a thorough understanding of R&M mechanisms at work will come creative solutions to increase Availability and reduce TCO.

Recall that Availability is defined as the probability that an item will be available when it is called upon for duty. Availability can also be thought of as the proportion of total time that an item is available for use. The underlying factors that influence availability are reliability and maintainability. Reliability is the probability that an item meets its intended function over a given timeframe and in a given environment. Maintainability is a measure of the ability to restore an item to a specified condition when a maintenance action is performed.

Three common measures of availability are Inherent Availability, Achieved Availability and Operational Availability. Inherent Availability is the ideal situation where the repair action occurs without delay, i.e. immediately when the item fails. Consequently, Inherent Availability is the simplest to model and is defined as:

$$A_i = \gamma / (\gamma + \lambda)$$

where γ = repair rate and λ = failure rate.

Assuming constant repair rate and constant failure rate, the simplified form of the Inherent Availability equation becomes:

$$A_i = MTBF / (MTBF + MTTR)$$

where MTBF is the mean time between failure and MTTR is the mean time to repair.

Achieved Availability is like Inherent Availability in that corrective maintenance actions are assumed to take place immediately upon failure. However, Achieved Availability also takes into account preventive maintenance actions. It is defined as:

$$A_a = MTBMA / (MTBMA + MMT)$$

where MTBMA is the mean time between both corrective and preventive maintenance actions and MMT is the mean maintenance action time.

Operational Availability best represents what is likely to occur in real life. It takes Achieved Availability one step further by accounting for the fact that most maintenance actions are not instantaneous, e.g. factors such as logistical delays in dispatching maintenance crews and delays in delivering replacement parts to repair depots. It is defined as

$$A_o = MTBMA / (MTBMA + MDT)$$

where MDT is the mean down time.

The example that follows employs Operational Availability methods.

Manufacturing of a New Microwave Device

Now let's turn our attention back to using Availability analysis methodologies to evaluate downtime mitigation strategies with the objective of minimizing TCO while still delivering on customer commitments.

We start by looking at a manufacturing operation that will produce a new microwave component. This new product is expected to be in manufacture for two years before being discontinued. Part of the manufacturing process includes final test where the device under test undergoes a complex suite of measurements. These tests are performed by an elaborate test system comprised of three measurement subsystem instruments (A, B and C) in which each has its own set of reliability characteristics. The Test System ABC is configured such that the subsystems are in series reliability-wise as shown in Figure 3.

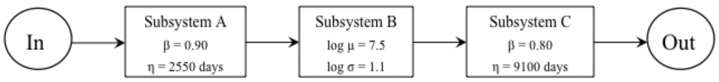

Figure 3. Reliability representation of Test System ABC.

Reliability characteristics for Test System ABC:

Subsystem A: 2-parameter Weibull distribution with shape parameter (β) = 0.9 and scale parameter (η) = 2550

Subsystem B: lognormal distribution with logmean (μ) = 7.5 and logstdev (σ) = 1.1

Subsystem C: 2-parameter Weibull distribution with shape parameter (β) = 0.8 and scale parameter (η) = 9100

The manufacturing floor is comprised of 20 identical but independently-operated Test Systems ABC as shown in Figure 4. The production process runs 24x7 and is 100% utilized. When one of the Test Systems goes down, the remaining 19 systems continue to run uninterrupted, however manufacturing output of the microwave device is temporarily lost until the failed system can be brought online again. For each minute of lost test time due to corrective maintenance, the enterprise loses $4.00 of gross margin (sometimes referred to as gross profit).*

* Gross margin = Net Sales minus Cost of Goods Sold

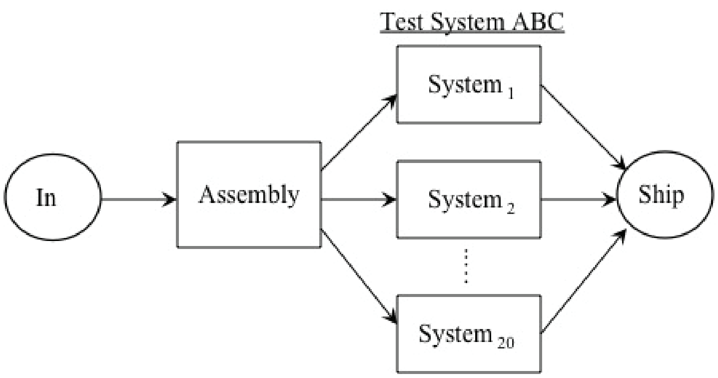

Figure 4. Manufacturing process flow.

Downtime Mitigation Strategies

Management has provided reliability engineering with the following four downtime mitigation scenarios for evaluation. They would like a recommendation for a strategy that minimizes TCO (as measured by impact on gross margin) and delivers on customer expectations.

Scenario 1: High Reliability

A special environmentally-controlled enclosure is designed and built to house the 20 test systems. Including procurement, installation, operating and energy costs, the total cost of the enclosure is $180,000. The residual value of the enclosure at the end of its useful life is $40,000. The enclosure results in improved reliability of the test systems with these reliability characteristics:

Subsystem A′: 2-parameter Weibull distribution with shape paraeter (β) = 0.95 and scale parameter (η) = 4000

Subsystem B′: lognormal distribution with logmean (μ) = 7.7 and logstdev (σ) = 1.0

Subsystem C′: 2-parameter Weibull distribution with shape parameter (β) = 0.85 and scale parameter (η) = 12000

Cost to have a failed system repaired is $20,000 and repair TAT is 10 days.

Scenario 2: Spare Test System

A complete spare test system is purchased and held in reserve. Cost is $320,000 and residual value after the end of its useful life is $60,000. When a system goes down, the spare system is deployed by technicians. The time required to deploy the spare system, verify performance characteristics and route production units to it is six hours. Cost to have a failed system repaired is $20,000 and repair TAT does not impact system availability.

Scenario 3: Offsite Annual Repair Contract

A third party service company is utilized. An annual repair contract is arranged whereby the failed system is shipped offsite for expedited repair. Cost of the annual contract is $180,000 per year to service the fleet of 20 test systems, and the downtime experienced during repair is five days.

Scenario 4: Onsite Repair

An arrangement is made with the equipment supplier to provide rapid response onsite repair of a downed test system. This is handled on a Per Incident basis and repair cost is $35,000 per event. The downtime in this scenario is 24 hours.

continued on next page ›››

continued from page 13

A summary of Investment (capital) expenses and Contract repair expenses for the four downtime mitigation strategies is shown in Table 1.

Reliability and Availability Analyses

Using the reliability characteristics of the subsystem components, the Test System reliability was calculated and charted over time as shown in Figure 5. One can see that the environmentally-controlled enclosure in Scenario #1 provides improved reliability as compared with the system reliability observed in the three other scenarios.

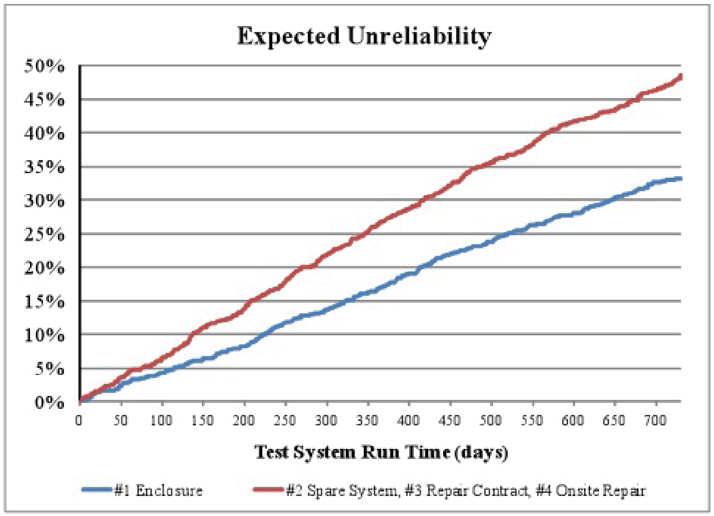

Figure 5. Unreliability curves generated from modeling system reliability of the four downtime mitigation strategies.

The reliability engineer then performed Availability analyses using the reliability and maintainability information provided in the four downtime mitigation strategies. Test system availability was modeled and expected outcomes were calculated using Monte Carlo simulation as shown in Figure 6.

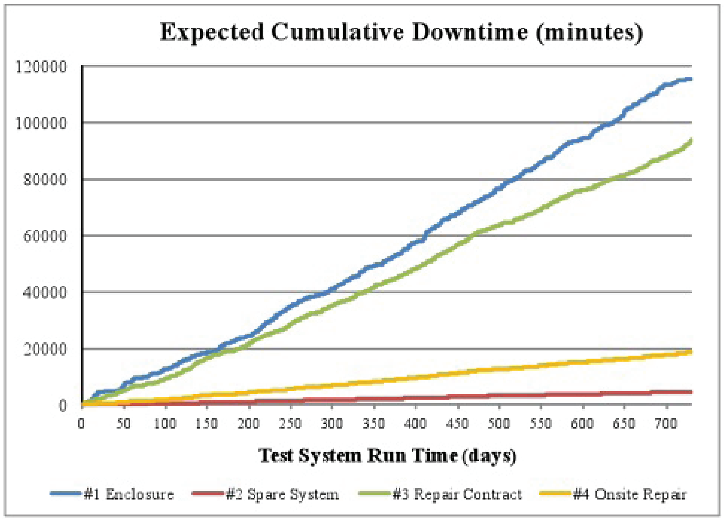

Figure 6. Expected total downtime of the 20 test systems under four different downtime mitigation strategies.

Based on the Availability analysis, the engineer calculates the expected number of failures and expected total downtime over a two year manufacturing lifecycle. Total repair costs were calculated by multiplying the expected number of failures times the Per Incident Repair costs listed earlier. The repair cost for Scenario #3 is zero because all repairs are covered under a service contract. Downtime costs were calculated by multiplying total expected downtime minutes times the impact on gross margin ($4.00 per downtime minute). Impact of operating costs on gross margins is then calculated by summing repairs costs and downtime costs as shown in Table 2.

Note: For each minute of lost test time due to corrective maintenance, the enterprise loses $4.00 of gross margin. This loss is reflected as Expected Downtime Costs and is calculated by multiplying Expected Downtime x $4.00.

By combining investment costs, repair contract costs and operating costs, we have the total impact on gross margins expected over the

Table 1. Investment and Contract expenses to implement downtime mitigation strategies.

Scenario	Downtime Mitigation Strategy	Investment Costs	Residual Value	Annual Contracted Repair Cost x 2	Total Invest. + Contract Costs
1	Enclosure	$180,000	$40,000	$ -	$140,000
2	Spare System	$320,000	$60,000	$ -	$260,000
3	Repair Contract	$ -	$ -	$360,000	$360,000
4	Onsite Repair	$ -	$ -	$ -	$ -

Table 2. Operational Availability, operating costs and impact on Gross Margins for the fleet of 20 test systems over the two year manufacturing lifecycle.

Scenario	Expected Op. Availability	Expected # of Failures	Expected Downtime (minutes)	Expected Repair Costs	Expected Downtime Costs	Impact of Op. Costs on Gross Margins
1	99.45%	8	115134	$160,000	$460,536	$620,536
2	99.98%	13	4677	$260,000	$18,708	$278,708
3	99.56%	13	92768	$ -	$371,072	$371,072
4	99.91%	13	18662	$455,000	$74,648	$529,648

two year manufacturing lifecycle of the new microwave component as shown in Table 3.

Table 3. Total impact on gross margin from the four downtime mitigation scenarios.

Scenario	Downtime Mitigation Strategy	Total Impact on Gross Margins
1	Enclosure	$760,536
2	Spare System	$538,708
3	Repair Contract	$731,072
4	Onsite Repair	$529,648

Through the incorporation of availability analysis with an understanding of TCO, we are able to develop a downtime mitigation strategy that minimizes costs to the organization and enables it to deliver on its customer commitments. In this hypothetical example, we see that purchasing a Spare Test System or establishing an Onsite Repair Agreement will provide the business with optimized results.

Conclusions

The costs to operate equipment over its useful life can easily exceed the capital expense used to acquire the equipment. Selecting an effective downtime mitigation strategy will help reduce the impact of unreliability on the business' bottom line. Performing availability analysis can be an essential step in selecting an optimal downtime mitigation strategy for reducing total cost of ownership.

Further Reading

1. "Operating and Support Cost-Estimating Guide", Cost Analysis Improvement Group, United States Department of Defense, May 1, 1992, Washington, DC.

2. "Uncovering the Total Cost of Ownership of Storage Management", Mark Buczynski, Computer Technology Review, January 2002, pp. 45-46.

3. "Practical Considerations in Calculating Reliability of Fielded Products", Bill Lycette, The Journal of the RAC, Second Quarter 2005, pp. 1-6.

4. "Total Cost of Ownership Models: An Exploratory Study", Bruce G. Ferrin and Richard E. Plank, Journal of Supply Chain Management, Summer 2002, pp. 18-29.

About the Author

Bill Lycette is a Quality Manager at Agilent Technologies in Santa Rosa, California. He has 29 years of experience in management, quality and reliability engineering, manufacturing engineering and NPI positions with Hewlett-Packard and Agilent Technologies. He is ASQ certified in Manager of Quality/Organizational Excellence and in Reliability Engineering. Mr. Lycette's undergraduate engineering study was in the field of materials science at the University of Washington and he holds an M.S. in Engineering Management from Stanford University.

The key to building reliable products

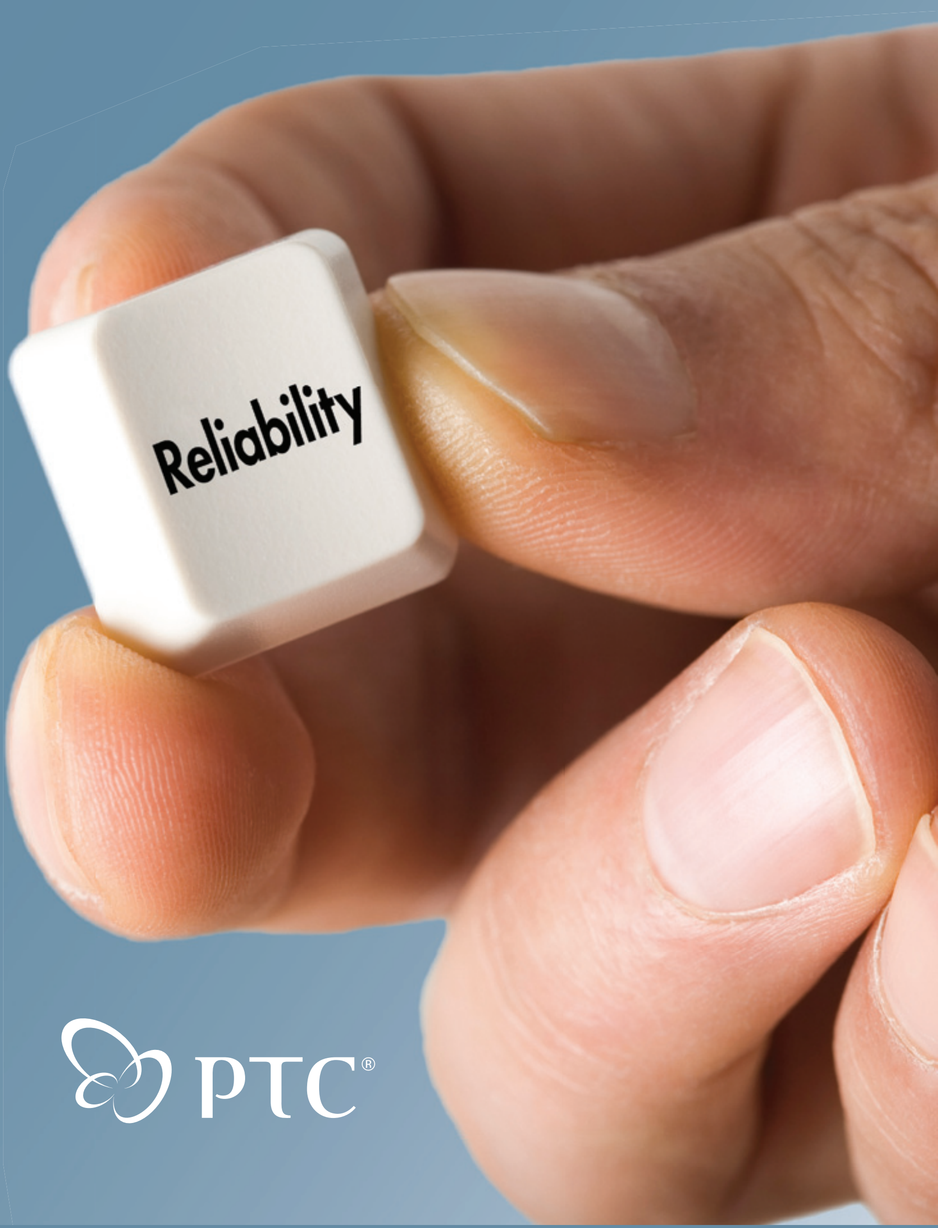

PTC®





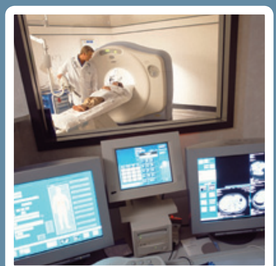

ability Prediction • Markov • OpSim • Reliability Prediction • Weibull

PLATFORM DEGRADER ANALYSIS FOR THE DESIGN AND DEVELOPMENT OF VEHICLE HEALTH MANAGEMENT SYSTEMS (VHMS)

Jeffrey C. Banks, Karl M. Reichard, Jason A. Hines and Mark S. Brought, Pennsylvania State University, Applied Research Laboratory

Degrader Analysis

The purpose of the degrader analysis is to ascertain where health monitoring technology would provide the greatest benefit through the implementation of the Condition-Based Maintenance (CBM) methodology. For U.S. Army Heavy Brigade Combat Team (HBCT) platforms the benefit is achieved by decreasing diagnostic time (increasing platform operational availability), increasing maintenance effectiveness, decreasing misdiagnosis/no evidence of failure conditions and facilitating the migration to a 2-tier maintenance system (only field or depot maintenance, with no intermediate level of maintenance support). In general, the degrader assessment aims to determine which platform components and sub-systems contribute the most toward vehicle lost operational availability; then identify diagnostic, predictive and prognostic technologies that are mature and appropriate to apply to these specific components and sub-systems. The greatest benefit can be achieved when the technology is applied to the degraders of the vehicles primary functions (mobility, armor, weapons, etc.). The determination and prioritization of the degraders of each vehicle type is determined through the assessment of the following questions as shown in Figure 1.

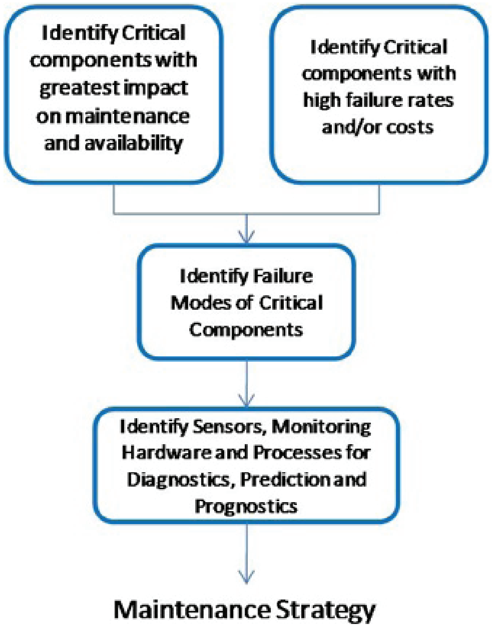

Figure 1: Degrader Analysis Process

The focus of this degrader analysis is to answer these questions through a systematic approach that enables the selection of the most effective health management technology and to determine where the application of the technology would provide the greatest benefit. The data and information that was gathered to answer these questions consisted of three types, including: part replacement data, maintainer interviews and an original equiptment manufacturer (OEM) questionnaire. Once the components and sub-systems that have the lowest reliability and greatest number of maintainability issues have been identified, then the next step in the degrader process is to evaluate how these components fail and determine their dominant and critical failure modes. This is accomplished using a FMECA on only the top degrader component and sub-systems. The final step in the degrader process identifies appropriate technology solutions for monitoring each dominant and critical failure mode, capable of providing an on-board diagnostic, predictive or prognostic assessment. These solutions are comprised of a basic methodology that first describes the observable symptoms related to the dominant modes of failure, and then provides the approaches that can be taken to monitor these observables with specific sensing technologies. This provides a list of sensors and diagnostic/predictive/prognostic approaches from which the on-platform health management system can be designed. Decision criteria can then be applied to determine which of the identified engineering solutions to implement. A very practical approach would involve the selection of the least number of sensors that would provide the broadest diagnostic and prognostic coverage. The coverage percentage can be quantified through the FMECA results by correlating the number of sensors applied to the number of failure modes. A degrader analysis for the M1 Abrams and M2/M3 Bradley was conducted to assess the top degraders of each vehicle's maintainability, reliability and operational availability (A_o). These vehicles will be used as examples for this paper.

Degrader Data Source 1: Part Replacement Data

In order to assess 'which parts are replaced most often' as a component reliability indicator; part replacement data was gathered from the OSMIS and LOGSA data bases. The first set of data was obtained from TACOM and it provided the top 10 repairables and consumables by total cost for the year 2006.

The tables provide an indication of which vehicle components or line replaceable units (LRU) are the highest cost drivers for each vehicle type for the year 2006. The tables provide the total number of LRU's that have been replaced, the total cost associated with each LRU and the cost per mile.

The next collection of part replacement data that was evaluated as a component reliability indicator was OSMIS data from the years 2002 to 2006 for the M1A1, M1A2, M2A2, M2A3, M3A2 and M3A3 platforms. The Operating and Support Management Information System (OSMIS) is the core of the Army Visibility and Management of Operating and Support Costs (VAMOSC) program. OSMIS tracks operating and support data of major Army weapon/materiel systems, and develops cost factors for the purpose of supporting a wide variety of analyses. OSMIS data can provide insight into the total quantity of parts obtained over a specified time period. This data does not necessarily reflect actual component failure rates, however it does clearly identify where O&S funds are being spent.

The third collection of part replacement data that was evaluated as a component reliability indicator was from the LOGSA Logistics Information Warehouse (LIW). The LIW contains data from the Integrated Logistics Analysis Program (ILAP) and the Army's Logistic Information Database (LIDB). Both databases contain records of dead-lining reports, and parts ordered against those repairs.

Table 1A: M1A2 Abrams Top Repairables

2006				M1A2 Abrams
Top 10 Repairables by Total Cost				
Nomenclature	Consumer	Qty.	Cost	Per Mile
ENGINE,GAS TURBINE,	256,431	291	$74,621,426.28	$134.84
TRANSMISSION,HYDRAULIC	59,121	137	$8,099,632.01	$14.64
WHEEL,SOLID RUBBER	315	6,964	$2,190,819.00	$3.96
FUEL SYSTEM ASSEMBLY	10,421	165	$1,719,406.66	$3.11
ELECTRONIC UNIT,FIR	46,696	31	$1,447,590.18	$2.62
SIGHT UNIT	48,491	26	$1,260,766.57	$2.28
GENERATOR,ENGINE AC	7,547	269	$2,030,223.53	$3.67
HEATER,VEHICULAR,CO	4,309	230	$991,139.68	$1.79
AZIMUTH DRIVE ASSEMBLY	11,913	77	$917,324.29	$1.66
COOLER-DEWAR GROUP	17,305	52	$899,843.79	$1.63

Table 1B: M2A2 Bradley Top Consumables

2006				M2A2 Bradley
Top 10 Consumables by Total Cost				
Nomenclature	Consumer	Qty.	Cost	Per Mile
BATTERY,NONRECHARGE	241	11,550	$2,787,547.62	$2.05
PARTS KIT,TRACK	10	197,057	$1,901,165.29	$1.40
SHOCK ABSORBER,BUMP	647	2,294	$1,485,338.84	$1.09
BARREL,MACHINE GUN	2,274	388	$882,400.06	$0.65
FEEDER,AUTOMATIC GU	6,957	113	$786,168.17	$0.58
CARRIER,SPROCKET DR	2,386	266	$634,784.64	$0.47
CIRCUIT CARD ASSEMB	1,860	336	$624,917.91	$0.46
PERISCOPE,ARMORED	251	2,390	$600,027.35	$0.44
SOLENOID SUBASSEMBLY	932	586	$546,250.55	$0.40
SENSOR,FIRE DETECT	1,188	429	$509,668.12	$0.38

Degrader Data Source 2: Customer Interviews

The second source of data and information for the degrader analysis was compiled results of interviews conducted with one of the primary VHMS customer groups: vehicle maintainers, field service representatives (FSR) and vehicle operators. The interviews consisted of a series of questions that are focused at gaining insight into vehicle component reliability, vehicle maintainability, maintainer effectiveness and platform operational availability issues. Three example questions included:

1. Which components or sub-systems fail or require unscheduled maintenance most often (list from most to least)?
2. Which subsystems require the most scheduled maintenance in terms of time spent conducting preventive maintenance checks and services (PMCS)? (Breakdown by sub-system was provided.)

2b. What is a typical amount of total time for conducting weekly PMCS paperwork (time and percentage)?

3. Which LRU's, components or sub-systems are the most difficult to troubleshoot for faults (Example: Weapons electronic circuit cards, final drive gear box, etc.)? Note: Specify troubleshooting information/technique issues for

continued on next page ›››

continued from page 19

this question and not physical design issues. (Breakdown by sub-system was provided.)

The results of the interviews for each platform were compiled and summarized with an emphasis on categorizing and prioritizing the data based on the issues that were consistently reported by the larger number of interviewees.

Degrader Data Source 3: Platform OEM Questionnaire

In order to provide an additional source of data and information for the degrader analysis, a questionnaire was developed for the OEMs to complete for Abrams and Bradley platforms. The focus of the questionnaires was to gather information about component reliability, component functionality, component criticality to the platform and maintainability issues for each of the major vehicle sub-systems and components as described by each platforms maintenance allocation chart (MAC).

The assessment analyses for each component or sub-system are based on seven factors including: Mission Criticality, Mission Reliability, On-Board Diagnostics, At-Platform Diagnostics, Time and Difficulty to Diagnose, Time and Difficulty to Repair and Relative Cost to Maintain.

This questionnaire is not intended to be a rigorous engineering reliability analysis. The primary purpose of the questionnaire is to provide a relative comparison of the vehicle components to each other for the selected factors, so that a general assessment of 'high opportunity' sub-systems and components can be evaluated for the degrader assessment. The course and broad ranking system was selected, so that the OEM can more quickly complete the questionnaire for use as a general reference.

Degrader Analysis – Systems for Focus

The top degrader components and sub-systems for each platform were selected based on analysis of three data sources including: the parts replacement data from the OSMSIS and LOGSA databases, the results of the interviews and the OEM questionnaire.

The results of the degrader analysis include a list of components and sub-systems that contribute most to maintainability, reliability and vehicle operational availability issues. The degrader list for the M1 Abrams is shown in Table 6.

Table 6: General Degrader List for the M1 Abrams Tank

M1 Abrams Top Degrader Components or Sub-Systems	2006 Total Cost for Repairables and Consumables from OSMIS (M1A1)	2006 Total Cost for Repairables and Consumables from OSMIS (M1A2)	Current Diagnostic Potential	Current Prognostic Potential	Future Diagnostic and Prognostic Potential
Turbine Engine	$154 MM	$75 MM	Yes	Possibly	Yes (Prog)
Transmission	$18 MM	$8 MM	Yes	No	Yes (Prog)
Batteries	NA	NA	No	No	Yes (Prog)
Suspension and Tracks	$58 MM	$24 MM	No	No	Possibly (Diag)
Hydraulic Pump	$3 MM	NA	No	No	Yes (Prog)
Cable Assembles and Wiring Harnesses	$2.5 MM	$1 MM	No	No	Yes (Diag)
Fire Control Electronic Unit	NA	$1.5 MM	Yes	No	No

The first 2 columns show the 2006 OSMIS repairable and consumable costs for the M1A1 and M1A2 respectively. The current diagnostic and prognostic potential columns indicate whether an automated diagnostic or prognostic capability exists or the sensor capability exists on the platform for the potential development. The future diagnostic or prognostic potential column indicates whether technology exists that could be applied to the platform to enable diagnostics or prognostics if it does not currently exist. If a future prognostic capability is indicated then a diagnostic capability is also implied, but if a future diagnostic capability is indicated then a prognostic capability is not implied. The diagnostic and prognostic assessments are general estimates that were conducted early in the program development; the potential for diagnostic and prognostic capabilities will change as we learn more about the platform systems, their failure mechanisms and as the diagnostic and prognostic technologies mature. The degrader list for the M2/M3 Bradley is shown in Table 7.

Table 7: General Degrader List for the M2/M3 Bradley Fighting Vehicle

M2/M3 Bradley Top Degrader Components or Sub-Systems	2006 Total Cost for Repairables and Consumables from OSMIS (M2A2 + M2A3)	2006 Total Cost for Repairables and Consumables from OSMIS (M3A2 + M3A3)	Current Diagnostic Potential	Current Prognostic Potential	Future Diagnostic and Prognostic Potential
Transmission	$30 MM	$7MM	No	No	Yes (Prog)
Batteries	$0.2 MM	NA	No	No	Yes (Prog)
Integrated Sight Assembly	$4.4 MM	$1.4MM	Yes	No	No (Prog)
Target Acquisition System	$2.5MM	$0.75MM	Yes	No	No (Prog)
Turret Drive Control Unit	$0.75MM	$0.25MM	Yes	No	No (Prog)
Turret Distribution Box	$2.5MM	$0.65MM	NA	No	No (Prog)
Suspension, Road Wheels, Sprockets and Tracks	$36.5MM	$11.4MM	No	No	Possibly (Diag)
Cable Assembles and Wiring Harnesses	$1.6MM	$0.17MM	No	No	Yes (Diag)
25mm Gun System	$0.78MM	$0.33MM	Yes	No	No (Prog)
Fuel Pumps	NA	NA	Yes	No	Yes (Prog)

The results of the degrader analysis provides the focus for the optimum development and application of embedded vehicle diagnostics and prognostics, which will enable the ability to implement a condition based maintenance methodology for more effective and efficient HCBT platform maintenance, logistic support and platform life cycle management.

Degrader Potential Solutions

The results of the vehicle degrader analysis was used to provide a focused list of specific systems and components for each platform type, for which VHMS could provide the greatest benefit in terms of increasing operational availability. The next portion of the analysis involved identifying sensors that could be utilized to enable an effective VHMS. An analysis was conducted using the degrader results that involved using field service representative reports for each platform type and the reliability centered maintenance (RCM) process known as failure modes, effects and criticality analysis (FMECA). This vehicle degrader solutions analysis provides a recommended list of sensors that either currently exist on the platform or would need to be added to enable a diagnostic or predictive capability for each degrader system or component.

Failure Modes, Effects and Criticality Analysis

The FMECA method is a RCM-based tool that is used for identifying, evaluating and prioritizing the functional failure modes of a system. When sensor information for each failure mode is identified as an addition to the standard FMECA format, then this evaluation tool can also be useful for the selection of sensors for the design of a system focused health management architecture. An example of the FMECA format that was used for this evaluation from the fuel system for the Bradley M2/M3 is shown in Figure 2.

The results of the FMECA will be used to facilitate the design of the VHMS architecture by identifying the sensors required to monitor for the dominant failure modes. The primary objective is to identify sensors that currently exist on the platform that could be used to monitor for each failure mode. When a sensor is not identified, an appropriate sensor is suggested. The completed FMECA provides a list of sensors that could be utilized to cover all of the dominant failure modes. The focus is to determine what are the least number of sensors that can be implemented to detect the greatest number of dominant failure modes. Those results and recommendations will be provided in this report for each specific component and sub-system that was evaluated. Based on the required failure mode coverage that is desired, the optimum selection of sensors for the platform embedded diagnostic, predictive and prognostic capability can be selected.

Function	Functional Failure Mode	Qualitative Probability Ranking	Severity Ranking	Symptoms/Effects	Component	Sensors	Diagnostics
The Bradley fuel system has two fuel tanks with a combined 175 gallons of usable diesel fuel. Fuel is supplied to the diesel engine by four electric fuel pumps mounted on the lower tank. Fuel flows through two check valves and a main shut-off valve then through the filter/water separator and then to the PT (pressure-time) pump that regulates the fuel pressure to the injectors with the electronic fuel control valve (EFCV). The PT pump provides fuel pressure between 129 psi - 163 psi depending on the pump used. Excess fuel is returned to the tank through a low pressure return line.	PT Pump Fault	A	I	Fuel rail pressure low	Engine	Rail Pressure Sensor	Trending
				Mis-diagnosed as transmission fault	Transmission	Rail Pressure Sensor	Sensor Fusion
				Loss/Decrease in Engine Power	Engine	*Throttle Position/Tachometer	Sensor Fusion
				Air-Fuel control (AFC) valve stuck?	Engine	Rail Pressure Sensor	Sensor Fusion
				Reduced vehicle speed capability	Engine	*Throttle Position/Tachometer	Sensor Fusion
				Engine exhibits erratic idle levels	Engine	*Throttle Position/Tachometer	Sensor Fusion
	PT Pump Accelerator Level Fault	D	III	Extreme high idle without operator input	Engine	*Throttle Position/Tachometer	Sensor Fusion
	Fuel Filter Restriction	C	III	Differential pressure out of range	Engine	Differential Pressure Sensor	Trending
				Mis-diagnosed as transmission fault	Transmission	Rail Pressure Sensor	Sensor Fusion
				Loss/Decrease in Engine Power	Engine	*Throttle Position/Tachometer	Sensor Fusion
	Electronic Fuel Control Valve (EFCV) failure	D	II	Loss/Decrease in Engine Power	Engine	*Throttle Position/Tachometer	Sensor Fusion
				Transmission does not shift	Transmission	Rail Pressure Sensor	Sensor Fusion
				Mis-diagnosed as transmission fault	Transmission	Rail Pressure Sensor	Sensor Fusion
	Fuel Leak (heater)	D	III	Excessive Fuel Smell	Compartment	Human Perception	Training
				Possible reduced fuel pressure	Heater	Pressure Sensor	Trending
	Air/Fuel Control (AFC) Valve Sticks	B	II	Engines stall	Engine	Rail Pressure Sensor	Sensor Fusion
				Inability to reach maximum speed	Engine	*Throttle Position/Tachometer	Sensor Fusion
				Valve command/response errors	Engine	*Throttle Position/Tachometer	Sensor Fusion
				Loss/Decrease in Engine Power	Engine	Rail Pressure Sensor	Sensor Fusion
	Vehicle Electric Distribution Box (VEDB) failure	D	I	Less than 17 volts supplied to fuel pumps	Engine	Fuel Tank Pump Voltage Sensor	Trending
				Fuel pumps are unable to function	Engine	Individual Voltage and Pressure Sensors	Sensor Fusion
				Engine is unable to function	Engine	Individual Voltage and Pressure Sensors	Sensor Fusion

Figure 2: FMECA Example for Bradley M2/M3 Fuel System

Bradley Degrader Solution Example: Fuel System

The FMECA for the Bradley fuel system lists eleven failure modes. It was determined based on the criticality portion of the analysis that three of the eleven could be considered 'high criticality' failure modes that warrant possible alleviation through the implementation of vehicle health management technology. The first failure mode will be discussed in more detail.

Arguably, the fuel system failure mode that has the greatest impact on vehicle functionality and the highest probability of occurrence based on the FSR report analysis is the pressure-time (PT) fuel pump. The PT fuel pump accounted for 17 out of 40 (43%) reported incidents from the fuel system portion of the FSR report. This is the high pressure fuel pump that provides fuel delivered from the fuel tank to the injectors and it is a single point of failure. The failure mode symptoms and effects with corresponding sensors that could be utilized to monitor for each symptom or effect are listed. The sensors listed with blue letters currently exist on the platform and the sensors listed in red are sensors that have been used with an at-platform STE system or are analog sensors that will require data conversion to digital.

Table 5: Effects and Sensors for PT Fuel Pump

Symptoms or Effects	Sensors
• Fuel rail pressure low	Fuel Rail Pressure Sensor
• Misdiagnosed as transmission fault	Fuel Rail Pressure Sensor
• Loss/Decrease in engine power	Throttle Position/Tachometer/XSMN Range
• Air-Fuel Control (AFC) Valve fault	Fuel Rail Pressure Sensor
• Reduced vehicle speed capability	Throttle Position/Tachometer/XSMN Range
• Engine exhibits erratic idle	Throttle Position/Tachometer/XSMN Range

The vehicle's current configuration does not utilize any sensors on the platform for conducting diagnostics specifically for the fuel system. A diagnostic capability could be enabled with the utilization of several existing vehicle signals including: throttle position, transmission range engaged and engine speed. These sensors could be used with a data fusion approach, which could be beneficial for conducting general fuel system diagnostics and potentially provide a predictive capability. This group of sensors could provide the ability to isolate a failure to the fuel system but it may not have the capability to isolate a failure to a specific component in the system (such as the PT pump). The ability to diagnose a failure and potentially predict a fault to the PT pump is dependant upon the ability to measure whether the pump pressure is within the specified operational range. In order to conduct basic diagnostics specifically for the pump, a pressure switch is sufficient but in order to provide a predictive capability a broad frequency bandwidth pressure transducer is required with supporting high sample rate data acquisition capability. The details for the development of a predictive capability for the PT fuel pump involve several steps. The first step is to identify the specific failure mechanisms of the pump (i.e. bearing failure, motor winding shorts, etc.). The next step is to develop early fault detection algorithms that are sensitive to the specific failure mechanism characteristic parameters (i.e. 2nd harmonic of the rotational speed vibration, bearing inner race fault frequency, etc.). In our experience, we have observed that many failure mechanism effects from a gear-driven or electric motor-driven pump can be detected in the broadband frequency pulsations of the pump flow stream. The predictive capability for the PT Pump could involve installing a broad bandwidth (3 to 20,000 Hz) capable pressure transducer in the pump outlet flow stream and supporting high sample rate (>40,000 Hz) data acquisition hardware. The hardware could apply time and frequency based analysis techniques to the raw pressure pulsation data to create condition indicators (CI) that are sensitive to specific failure mechanisms. Once the fault evolu-

continued on next page ›››

continued from page 21

tion effects on the CI's are characterized, the CI's can be trended over time against established detection and failure thresholds to provide a predictive fault indication as shown in Figure 3.

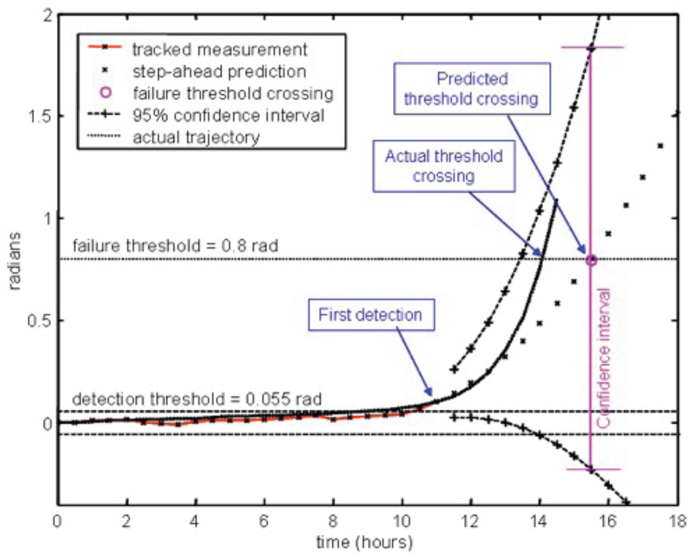

Figure 3: Condition Indicator Trending Against Defined Thresholds

The thresholds can be determined by several different means including statistical-based and physics model-based methods. The effectiveness of the prediction is dependant upon access to available data for the generation, training and testing of the CI's, threshold levels and the projection algorithms/models.

A generalized and estimated comparative description of the differences between the VHMS capabilities for the PT fuel pump is provided in Table 6.

Table 6: VHMS Capability Description for the PT Fuel Pump

PT Fuel Pump		Sensors: Quantity	Sensors: Type	Hardware Required	Software Required	Health Coverage	Logistic Benefit
Based on the Data from the FSR Report: the PT Fuel Pump accounts for 17 of 40 (43%) of the fuel system failures.	Current Capability	0	None are currently used for this application	Not Required	Not Required	0%	No
		0					
		0					
	Diagnostic	1	Throttle	Low Complexity	Low Complexity	50%	No
		1	Transmission Range Engaged				
		1	Engine Speed				
	Predictive	1	Throttle	High Complexity	High Complexity	95%	Yes
		1	Transmission Range Engaged				
		1	Engine Speed				
		1	Pressure Sensor				

The VHMS capabilities listed for each fault are presented in tables in which the rows of the table include three categories: the existing capability on the platform to provide health monitoring for the specified component, expanded diagnostic capability (which would require the addition of hardware and software), and a predictive capability (which would require the addition of sensors, additional data acquisition and processing technology, advanced algorithms and software).

The health coverage column provides an approximate indication of the percentage of the failure modes/mechanisms that each VHMS capability could detect. This percentage was extracted from the FSR report and FMECA results and it provides a coarse estimate of the impact for each capability level. Though in some cases, there may not be a dramatic health coverage difference between the diagnostic and predictive capabilities; the significant difference between the capabilities occurs through the logistic benefit. The logistics benefit for the predictive capability is the potential to plan for maintenance activities while the platform is still functional, which could have a direct impact on platform operational availability. This benefit will be more fully realized when this data is applied to the cost benefit analysis model [4] which is described in another publication.

Conclusion

The degrader analysis results for each platform provide a defined path forward to determine where the implementation of embedded diagnostics and prognostics would provide the greatest benefit in terms of increasing maintenance efficiency, effectiveness and vehicle A_o. The components and sub-systems listed in the degrader results provide the focus for the implementation of the VHMS technology.

Acknowledgment

Jeffrey Banks thanks the invaluable support provided by Gerald Biolchini at PM-HBCT, Dr. Brian Van De Wal at Benet Laboratory and Joe Wysocki & Gary Kempen at Control Point Corporation for this effort.

References

1. G. Grossman, "U.S. Army CBM+ Roadmap", Deputy Chief of staff, G-4, Headquarters, Department of the Army, 13 December 2007.

2. *Military Standard System Safety Program Requirements (MIL-STD-882C)*, 3rd Edition, Department of Defense, AMSC Number F6861, 19 January 1993,

3. *Technical Manual (TM 9-2350-294-20-1-1)*, Commander, U.S. Army Tank-automotive and Armaments Command, ATTN: AMSTA-LC-CLB, Warren, MI 48397--5000.

4. Jason Hines, Lorri Bennett, Chris Ligetti, Jeff Banks & LTC Scott Nestler, 'Cost-Benefit Analysis Trade-Space Tool as a Design-Aid for the U.S. Army Vehicle Health Management System (VHMS) Program', PHM Conference 2009

DISCRETE RELIABILITY GROWTH TRACKING

Vito Faraci Jr

Introduction

Reliability growth is the improvement in reliability over a period of time due to changes in product design or a manufacturing process. This occurs by performing root cause analysis of failures detected during testing, and implementing effective corrective actions.

Typical reliability growth testing involves the use of times-to-failure data obtained from the device testing during development. However, many products or systems, such as rockets and missiles, may not produce times-to-failure data because they are one time usage (or one-shot) devices. Such devices require algorithms different from the ones used to analyze times-to-failure data.

Motivation

MIL-HDBK 189A entitled "Department of Defense Handbook Reliability Growth Management" deals with the science of calculating Reliability Growth. It is very detailed and is the result of years of hard work and study. However, its treatment of "one shot" devices, sometimes referred to as discrete devices, utilizing the AMSAA / Crow Discrete Reliability Growth Tracking Model (algorithm) is somewhat difficult to follow. In my last article, entitled "Measuring Failure Rates by Testing" I presented an industry standard algorithm (equation) that is used by major IC manufacturing companies to measure failure rates of ICs. This algorithm uses times-to-failure data obtained from device testing. The article's objective was to reveal the algorithm's foundation (pure and basic probability theory) so one could more easily understand how and why it works. It turns out that this same algorithm, with some minor modifications, can also be used to measure reliability of "one shot" devices. Not only is this proposed methodology easier to understand, but it is also desirably more flexible than the AMSAA / Crow method which is the motivation for this article.

The Chi-Square Algorithm

The excerpt below illustrates an industry standard method for calculating maximum failure rate (λ_{MAX}) of electrical devices utilizing a Chi-Square ($\chi 2$) Distribution Algorithm. The quantitative inputs to this algorithm are the number of devices (usually ICs) being tested, the number of hours under test, the number of failures detected, and α (confidence level in percent). The output is the maximum failure rate (minimum MTTF) of the device associated with a specified α where T = number of devices being tested (n) times the number of hours under test (t) i.e. T = n · t.

Excerpt from National Semiconductor (Chi-Square Algorithm)

$$\lambda_{MAX} = \frac{\chi^2_{1-\alpha}[\textit{with}\ \mathrm{df} = 2(\mathrm{r}+1)]}{2T}$$

Maximum Failure Rate or worst case where:

$\chi 2$ = Chi-Square Distribution
r = Number of Failures
df = Degrees of freedom
T = Total number test hours (number of devices x number of hours)
α = Statistical error expected in estimate. For 60% confidence level, α = 0.6

Alpha can then be interpreted to mean that we can state with statistical confidence level of alpha (i.e., 60%) that the actual failure rate is equal to or less than the calculated maximum (λ_{MAX}) failure rate.

Small Modification

Assuming the above algorithm valid, it is modified as follows: Since T = n·t = number of devices x number of hours, we replace T with n·t and get:

$$\lambda_{MAX} = \frac{\chi^2_{1-\alpha}[\,df = 2(r+1)]}{2T} \Rightarrow \lambda_{MAX}$$

$$= \frac{\chi^2_{1-\alpha}[\,df = 2(r+1)]}{2nt} \Rightarrow \lambda_{MAX} \cdot t$$

$$= \frac{\chi^2_{1-\alpha}[df = 2(r+1)]}{2n}$$

Assuming an exponential characteristic of failure, the equation for probability of failure (q) is $q = 1-e^{-\lambda t}$ where λ = failure rate and t = exposure time. It can be proven that if q is small, $q = 1-e^{-\lambda t} \approx \lambda t$.

(See Appendix for a proof of this and a discussion on the expected error.) Substituting q for λt we get $q_{MAX} = \lambda_{MAX} \cdot t = \frac{\chi^2_{1-\alpha}[df = 2(r+1)]}{2n} \Rightarrow$

Modified Chi Square Algorithm

$q_{MAX} = \frac{\chi^2_{1-\alpha}[with\ df = 2(r+1)]}{2n}$ Maximum Probability of Failure or worst case where:

χ2 = Chi-Square Distribution
r = Number of Failures
df = Degrees of freedom
n = Total number of trials
α = Statistical error expected in estimate. For 60% confidence level, α = 0.6

Alpha can then be interpreted to mean that we can state with statistical confidence level of alpha (i.e., 60%) that the actual probability of failure is equal to or less than the calculated maximum (q_{MAX}) probability of failure.

Note: Since $Rel_{MIN} = 1-q_{MAX}$ the above could also be stated in terms of Rel_{MIN}

Basic Algorithm (Assuming 90% Confidence Level)

To illustrate this modified algorithm in its very basic form, consider the following example where 6 trial tests are performed, and all trials pass except for trial 4 (see chart below). Columns 1 and 2 keep track of trials and pass/fail score for each trial as shown. Note that r is the cumulative number of failures that occur, and df = 2(r+1) as shown in Columns 3 and 4. Column 5 is a Chi-Square Table look-up using α = 0.9 (see Appendix), and Column 6 (q_{MAX}) is simply Column 5 divided by 2n. Finally Column 7 (Rel_{MIN}) is simply 1–Column 6. So it is obvious that data entry is quite simple and easy to compile using a spreadsheet.

1	2	3	4	5	6	7
n (Trial #)	Pass / Fail	r	df 2(r+1)	$\chi^2_{0.1}[df]$ (Table look-up)	$q_{MAX} = \frac{\chi^2_{0.1}[df]}{2n}$	Rel_{MIN} = 1-q_{MAX}
1	Pass	0	2	4.6052	2.3026	-1.3026
2	Pass	0	2	4.6052	1.1513	-0.1513
3	Pass	0	2	4.6052	0.7675	0.2325
4	Fail	1	4	7.7794	0.9724	0.0276
5	Pass	1	4	7.7794	0.7779	0.2221
6	Pass	1	4	7.7794	0.6483	0.3517

Taking Appropriate Credits/Discredits with Failure Root Cause Analysis

In order to measure device reliability as accurately as possible, a root cause analysis should be performed after every failure. Root cause analyses will reveal various causes of failure which may or may not be due to the design flaws. Consider the following cases:

Case 1 - Human Error

Root cause analysis of a failure determined that a technician loaded incorrect software into a device prior to testing. In such a case, the trial should be discounted.

When measuring device reliability, human error should not be counted towards a device failure. Probability of human error should be considered separately from hardware/software reliability.

Case 2 – 100% confidence of fix

Root cause of failure was determined and a fix put in place resulting in 100% confidence that the particular failure could not occur again. For example it is determined that an incorrect part was installed in a device due to a Bill of Material typo. Again, in such a case, the failure should be discounted.

Note: Some engineering judgment is required here. If it is determined positively that the device would have indeed passed its test if the correct part was installed, consideration should be made for taking credit for that trial.

Case 3 – xx% confidence of fix

Root cause of failure is determined and fix put in place resulting in xx% confidence that the particular failure cannot occur again. For example, engineering implements a fix with a 65% confidence that the failure will not occur again. Instead of taking total discredit for the failure, consideration should be made for taking 65% credit for that trial which is equivalent to taking a discredit of 0.35 failures. The modified algorithm is designed to handle partial failure representations. This allows for taking partial credit or discredit for a failure.

Case 4 – Root cause of failure cannot be determined. In this case, no credit should be taken.

Due to the fact that all the above cases (scenarios) do commonly occur, it is desirable that an algorithm be capable of allowing the user to input partial credit or discredit for any given failure.

continued on next page ›››

continued from page 25

Example 1: *(90% Confidence, Initial Reliability 0%) (See explanation of negative entry)*

R(initial)	n	Pass/Fail	FIX % Conf.	r	df	Chi Sq	Q	Rel
0								
	1	Pass		0	2	4.6052	1.1513	-0.1513
	2	Pass		0	2	4.6052	0.7675	0.2325
	3	Pass		0	2	4.6052	0.5756	0.4244
	4	Fail	60	0.4	2.8	5.9221	0.5922	0.4078
	5	Pass		0.4	2.8	5.9221	0.4935	0.5065
	6	Pass		0.4	2.8	5.9221	0.4230	0.5770
	7	Fail	75	0.65	3.3	6.7098	0.4194	0.5806
	8	Pass		0.65	3.3	6.7098	0.3728	0.6272
	9	Pass		0.65	3.3	6.7098	0.3355	0.6645
	10	Pass		0.65	3.3	6.7098	0.3050	0.6950
	11	Pass		0.65	3.3	6.7098	0.2796	0.7204
	12	Pass		0.65	3.3	6.7098	0.2581	0.7419
	13	Pass		0.65	3.3	6.7098	0.2396	0.7604
	14	Pass		0.65	3.3	6.7098	0.2237	0.7763
	15	Pass		0.65	3.3	6.7098	0.2097	0.7903
	16	Fail	90	0.75	3.5	7.0154	0.2063	0.7937
	17	Pass		0.75	3.5	9.9405	0.1949	0.8051
	18	Pass		0.75	3.5	9.9405	0.1846	0.8154
	19	Fail	0	1.75	5.5	9.9405	0.2485	0.7515
	20	Pass		1.75	5.5	9.9405	0.2367	0.7633
	21	Pass		1.75	5.5	9.9405	0.2259	0.7741
	22	Pass		1.75	5.5	9.9405	0.2161	0.7839
	23	Pass		1.75	5.5	9.9405	0.2071	0.7929
	24	Pass		1.75	5.5	9.9405	0.1988	0.8012
	25	Pass		1.75	5.5	9.9405	0.1912	0.8088
	26	Fail	100	1.75	5.5	9.9405	0.1841	0.8159
	27	Pass		1.75	5.5	9.9405	0.1775	0.8225
	28	Pass		1.75	5.5	9.9405	0.1714	0.8286
	29	Pass		1.75	5.5	9.9405	0.1657	0.8343
	30	Pass		1.75	5.5	9.9405	0.1603	0.8397
	31	Pass		1.75	5.5	9.9405	0.1553	0.8447
	32	Pass		1.75	5.5	9.9405	0.1506	0.8494
	33	Pass		1.75	5.5	9.9405	0.1462	0.8538
	34	Pass		1.75	5.5	9.9405	0.1420	0.8580
	35	Pass		1.75	5.5	9.9405	0.1381	0.8619
	36	Pass		1.75	5.5	9.9405	0.1343	0.8657
	37	Pass		1.75	5.5	9.9405	0.1308	0.8692
	38	Pass		1.75	5.5	9.9405	0.1274	0.8726
	39	Pass		1.75	5.5	9.9405	0.1243	0.8757
	40	Pass		1.75	5.5	9.9405	0.1212	0.8788
	41	Pass		1.75	5.5	9.9405	0.1183	0.8817
	42	Pass		1.75	5.5	9.9405	0.1156	0.8844
	43	Pass		1.75	5.5	9.9405	0.1130	0.8870

Example 1A: *(90% Confidence, Initial Reliability 70%)*

R(initial)	n	Pass/Fail	FIX % Conf.	r	df	Chi Sq	Q	Rel
0.7								
	1	Pass		0	2	4.6052	0.3289	0.6711
	2	Pass		0	2	4.6052	0.2878	0.7122
	3	Pass		0	2	4.6052	0.2558	0.7442
	4	Fail	60	0.4	2.8	5.9221	0.2961	0.7039
	5	Pass		0.4	2.8	5.9221	0.2692	0.7308
	6	Pass		0.4	2.8	5.9221	0.2468	0.7532
	7	Fail	75	0.65	3.3	6.7098	0.2581	0.7419
	8	Pass		0.65	3.3	6.7098	0.2396	0.7604
	9	Pass		0.65	3.3	6.7098	0.2237	0.7763
	10	Pass		0.65	3.3	6.7098	0.2097	0.7903
	11	Pass		0.65	3.3	6.7098	0.1973	0.8027
	12	Pass		0.65	3.3	6.7098	0.1861	0.8136
	13	Pass		0.65	3.3	6.7098	0.1766	0.8234
	14	Pass		0.65	3.3	6.7098	0.1677	0.8323
	15	Pass		0.65	3.3	6.7098	0.1598	0.8402
	16	Fail	90	0.75	3.5	7.0154	0.1594	0.8406
	17	Pass		0.75	3.5	7.0154	0.1525	0.8475
	18	Pass		0.75	3.5	7.0154	0.1462	0.8538
	19	Fail	0	1.75	5.5	9.9405	0.1988	0.8012
	20	Pass		1.75	5.5	9.9405	0.1912	0.8088
	21	Pass		1.75	5.5	9.9405	0.1841	0.8159
	22	Pass		1.75	5.5	9.9405	0.1775	0.8225
	23	Pass		1.75	5.5	9.9405	0.1714	0.8286
	24	Pass		1.75	5.5	9.9405	0.1657	0.8343
	25	Pass		1.75	5.5	9.9405	0.1603	0.8397
	26	Fail	100	1.75	5.5	9.9405	0.1553	0.8447
	27	Pass		1.75	5.5	9.9405	0.1506	0.8494
	28	Pass		1.75	5.5	9.9405	0.1462	0.8538
	29	Pass		1.75	5.5	9.9405	0.1420	0.8580
	30	Pass		1.75	5.5	9.9405	0.1381	0.8619
	31	Pass		1.75	5.5	9.9405	0.1343	0.8657
	32	Pass		1.75	5.5	9.9405	0.1308	0.8692
	33	Pass		1.75	5.5	9.9405	0.1274	0.8726
	34	Pass		1.75	5.5	9.9405	0.1243	0.8757
	35	Pass		1.75	5.5	9.9405	0.1212	0.8788
	36	Pass		1.75	5.5	9.9405	0.1183	0.8817
	37	Pass		1.75	5.5	9.9405	0.1156	0.8844
	38	Pass		1.75	5.5	9.9405	0.1130	0.8870
	39	Pass		1.75	5.5	9.9405	0.1104	0.8896
	40	Pass		1.75	5.5	9.9405	0.1080	0.8920
	41	Pass		1.75	5.5	9.9405	0.1057	0.8943
	42	Pass		1.75	5.5	9.9405	0.1035	0.8965
	43	Pass		1.75	5.5	9.9405	0.1014	0.8986

Basic Algorithm with Added Features

1. Allows for partial credit (discredit) of failures when engineering judgment calls for it, i.e. percent confidence of fixes.
2. Allows for user input of initial reliability.

Example 1 illustrates reliability growth tracking with 43 trials calculated at a 90% confidence level. Five failures were detected, a root cause analysis was performed after each failure, and a fix put in place whenever the root cause was determined. Note how the algorithm handles partial credit/discredit for failures. If an xx% fix confidence is established, instead of counting one whole failure, (100− xx)% of the failure is counted.

Explanation of Negative Probability Entry

Initial negative probability entries are a result of the nature of the Chi-Square Algorithm itself and the % Confidence factor selected. The output of negative probabilities is simply the algorithm's way of indicating that there is not enough input data present. These negative entries can easily be replaced by zeroes, but this will only be a cosmetic fix and would not add to the algorithm's accuracy. From a mathematical point of view the negative readings may be desired and can be left on the chart. From a practical point of view zeros may be more desirable. This should be left to the analyst's discretion.

Definition: Confidence Level is a percentage measure of times test results can be expected to be within a specified interval.

Therefore in the Rel Growth Spreadsheets above, one can expect a percentage measure of times that the variable λ will be found in an interval. This is mathematically represented as $P(0 \le \lambda \le \lambda_{MAX}) = 0.9$ where 0.9 represents 90% probability.

Code for Excel Spreadsheet used to generate Examples 1 and 1A:

Name	Column	Code / Entry
n	B	Enter trial number n
Pass/Fail	C	Enter Pass / Fail
Fix % Conf	D	Enter confidence of fix
df	F	=2*ER+2
Chi Sq	G	=(CHIINV(0.1,INT(FR))+(FR-INT(FR))*(CHIINV(0.1,INT(FR)+1)−CHIINV(0.1,INT(FR))))
Q	H	=GR/2/(BR+$N$2−1)
Rel	I	=1−HR

Note: R= row numbers 4 thru 46. So for example fill Column F with =2*E4+2 thru =2*E46+2

Name	Cell	Code / Entry	Notes
Init Rel	A3	Enter Rel Initial	
	N2	=INT(CHIINV(0.1,2)/2/(1−$A$3))	used for initial rel calculation
r	E4-E6	0	r = 0
r	E7-E9	=(100−$D$7)/100	first failure appears in row 7
r	E10-E18	=$E$9+(100−$D$10)/100	second failure appears in row 10
r	E19-E21	=$E$18+(100−$D$19)/100	third failure appears in row 19
r	E22-E28	=$E$21+(100−$D$22)/100	fourth failure appears in row 22
r	E29-E46	=$E$28+(100−$D$29)/100	fifth failure appears in row 29

Notes: Column E has to be filled manually. Note that Column E entries remain the same until a failure occurs.

Graph of Examples 1 and 1A above showing the effect of differing initial reliability

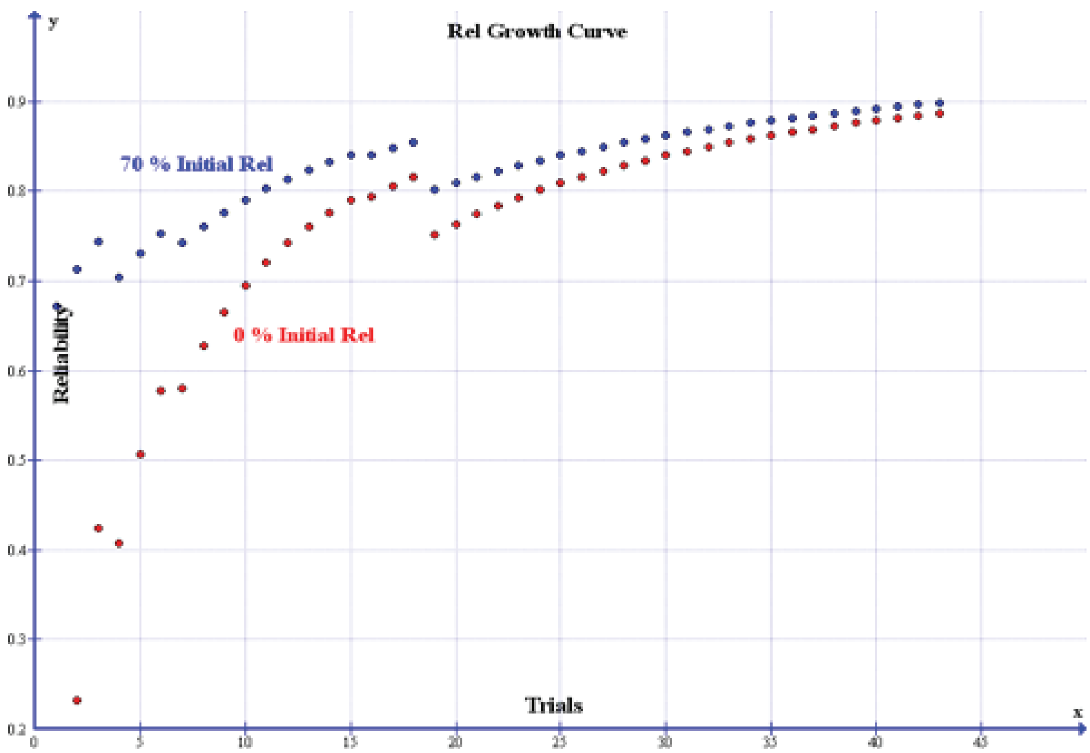

Note: Recall this entire methodology is based on pure and basic Probability theory.

continued on next page ›››

continued from page 27

Discussion on Expected Error

λt = Lambda x time is an approximation for $1\text{-}e^{-\lambda t}$ when λt is small. As far as the accuracy of this approximation tool refer to the table below. As an example $\lambda t = 0.1666$ Þ 8.56% error. With respect to missiles and rockets, t (exposure time) may only be for seconds or minutes. So for example to get some perspective, let us take a missile with a one minute exposure time (t = 1/60 hours). Then calculate a value of lambda required to yield a product of 0.166. 0.166 $= \lambda t = \lambda/60/10^6$ Þ λ = 10 failures per hour or 10 million FPMH. This implies a very poor design which is not realistic. Let us now take a more realistic lambda like 1000 FPMH, then $\lambda t = 1000/60/10^6$ = .00001666666666666 Þ $1\text{-}e^{-\lambda t}$ = 0.0000166665277785416 which yields an expected error of 0.00083% which is negligible.

FPMH vs. Expected % Error Chart
(based on a one minute exposure time)

FPMH (t=1min)	% Error	λt (Lambda x time)	1-e^(-λt)
50,000,000	47.38781268	0.833333333333	0.56540179149292200000
10,000,000	8.564707718	0.166666666667	0.15351827510938600000
5,000,000	4.22453034	0.083333333333	0.07995558537067670000
1,000,000	0.835648137	0.016666666667	0.01652854617838250000
500,000	0.41724537	0.008333333333	0.00829870736112404000
100,000	0.083356481	0.001666666667	0.00166527854906129000
50,000	0.041672454	0.000833333333	0.00083298620754168600
10,000	0.008333565	0.000166666667	0.00016665277854932500
5,000	0.004166725	0.000083333333	0.00008332986120751510
1,000	0.000833336	0.000016666667	0.00001666652777854160
500	0.000416668	0.000008333333	0.00000833329861116283
100	8.33328E-05	0.000001666667	0.00000166666527778858

CORRECTION

There was an error in the article titled "**Using Cost and Schedule Estimates to Plan Efficient, Coordinated Programs of Reliability Growth and Qualification Testing**" by David Lee and E. Andrew Long appearing on page 6 of the **4th Quarter 2009 journal**. Equation number 12 should be as follows:

$$T_{TAAF} = \frac{1}{\beta}\,\frac{\lambda_i + \lambda_A - \lambda_n^*}{\lambda_n^* - \lambda_A - \lambda_i(1-\mu_d)}$$

THE JOURNAL OF THE RELIABILITY INFORMATION ANALYSIS CENTER // SECOND QUARTER - 2010

The Journal of the Reliability Information Analysis Center is published quarterly by the Reliability Information Analysis Center (RIAC). The RIAC is a DoD Information Analysis Center (IAC) sponsored by the Defense Technical Information Center (DTIC) and operated by a team led by Wyle Laboratories, and including Quanterion Solutions Incorporated, the Center for Risk and Reliability at the University of Maryland, the Penn State University Applied Research Lab (ARL) and the State University of New York Institute of Technology (SUNYIT).

The Reliability Information Analysis Center
100 Seymour Road
Suite C101
Utica, NY 13502-1348
Toll Free: 877.363.RIAC (7422)
P 315.351.4200 // FAX 315.351.4209
inquiry@theRIAC.org
http://theRIAC.org

RIAC Journal Editor, David Nicholls
Toll Free: 877.363.RIAC (7422)
P 315.351.4202 // FAX 315.351.4209
dnicholls@theRIAC.org

Appendix

Chi-Square Distribution Table

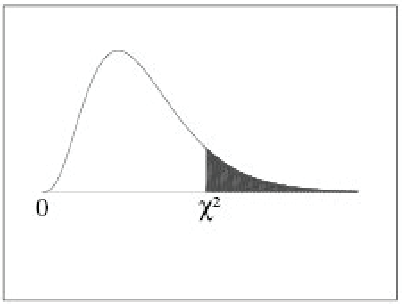

The shaded area is equal to α for $\chi^2 = \chi^2_\alpha$.

df	$\chi^2_{.995}$	$\chi^2_{.990}$	$\chi^2_{.975}$	$\chi^2_{.950}$	$\chi^2_{.900}$	$\chi^2_{.100}$	$\chi^2_{.050}$	$\chi^2_{.025}$	$\chi^2_{.010}$	$\chi^2_{.005}$
1	0.000	0.000	0.001	0.004	0.016	2.706	3.841	5.024	6.635	7.879
2	0.010	0.020	0.051	0.103	0.211	4.605	5.991	7.378	9.210	10.597
3	0.072	0.115	0.216	0.352	0.584	6.251	7.815	9.348	11.345	12.838
4	0.207	0.297	0.484	0.711	1.064	7.779	9.488	11.143	13.277	14.860
5	0.412	0.554	0.831	1.145	1.610	9.236	11.070	12.833	15.086	16.750
6	0.676	0.872	1.237	1.635	2.204	10.645	12.592	14.449	16.812	18.548
7	0.989	1.239	1.690	2.167	2.833	12.017	14.067	16.013	18.475	20.278
8	1.344	1.646	2.180	2.733	3.490	13.362	15.507	17.535	20.090	21.955
9	1.735	2.088	2.700	3.325	4.168	14.684	16.919	19.023	21.666	23.589
10	2.156	2.558	3.247	3.940	4.865	15.987	18.307	20.483	23.209	25.188
11	2.603	3.053	3.816	4.575	5.578	17.275	19.675	21.920	24.725	26.757
12	3.074	3.571	4.404	5.226	6.304	18.549	21.026	23.337	26.217	28.300
13	3.565	4.107	5.009	5.892	7.042	19.812	22.362	24.736	27.688	29.819
14	4.075	4.660	5.629	6.571	7.790	21.064	23.685	26.119	29.141	31.319
15	4.601	5.229	6.262	7.261	8.547	22.307	24.996	27.488	30.578	32.801
16	5.142	5.812	6.908	7.962	9.312	23.542	26.296	28.845	32.000	34.267
17	5.697	6.408	7.564	8.672	10.085	24.769	27.587	30.191	33.409	35.718
18	6.265	7.015	8.231	9.390	10.865	25.989	28.869	31.526	34.805	37.156
19	6.844	7.633	8.907	10.117	11.651	27.204	30.144	32.852	36.191	38.582
20	7.434	8.260	9.591	10.851	12.443	28.412	31.410	34.170	37.566	39.997
21	8.034	8.897	10.283	11.591	13.240	29.615	32.671	35.479	38.932	41.401
22	8.643	9.542	10.982	12.338	14.041	30.813	33.924	36.781	40.289	42.796
23	9.260	10.196	11.689	13.091	14.848	32.007	35.172	38.076	41.638	44.181
24	9.886	10.856	12.401	13.848	15.659	33.196	36.415	39.364	42.980	45.559
25	10.520	11.524	13.120	14.611	16.473	34.382	37.652	40.646	44.314	46.928
26	11.160	12.198	13.844	15.379	17.292	35.563	38.885	41.923	45.642	48.290
27	11.808	12.879	14.573	16.151	18.114	36.741	40.113	43.195	46.963	49.645
28	12.461	13.565	15.308	16.928	18.939	37.916	41.337	44.461	48.278	50.993
29	13.121	14.256	16.047	17.708	19.768	39.087	42.557	45.722	49.588	52.336
30	13.787	14.953	16.791	18.493	20.599	40.256	43.773	46.979	50.892	53.672
40	20.707	22.164	24.433	26.509	29.051	51.805	55.758	59.342	63.691	66.766
50	27.991	29.707	32.357	34.764	37.689	63.167	67.505	71.420	76.154	79.490
60	35.534	37.485	40.482	43.188	46.459	74.397	79.082	83.298	88.379	91.952
70	43.275	45.442	48.758	51.739	55.329	85.527	90.531	95.023	100.425	104.215
80	51.172	53.540	57.153	60.391	64.278	96.578	101.879	106.629	112.329	116.321
90	59.196	61.754	65.647	69.126	73.291	107.565	113.145	118.136	124.116	128.299
100	67.328	70.065	74.222	77.929	82.358	118.498	124.342	129.561	135.807	140.169

continued on next page ›››

continued from page 29

Theorem

$$\lim_{x \to 0} \frac{1 - e^{-x}}{x} = 1$$

Proof using L'hopital's Rule

L'hopital's Rule : *If* a) $\lim_{x \to 0} f(x) = 0$ and $\lim_{x \to 0} g(x) = 0$ and b) $\lim_{x \to 0} \frac{f'(x)}{g'(x)}$ exists, then $\lim_{x \to 0} \frac{f(x)}{g(x)} = \lim_{x \to 0} \frac{f'(x)}{g'(x)}$

Let $f(x) = 1 - e^{-x}$ and $g(x) = x \Rightarrow f(0) = 0$ and $g(0) = 0$ satisfies condition a)

$f'(x) = e^{-x}$, $g'(x) = 1 \Rightarrow \frac{f'(x)}{g'(x)} = e^{-x} \Rightarrow \frac{f'(x)}{g'(x)}$ exists satisfies condition b) $\Rightarrow$

$$\lim_{x \to 0} \frac{f(x)}{g(x)} = \lim_{x \to 0} \frac{f'(x)}{g'(x)} = \lim_{x \to 0} \frac{e^{-x}}{1} = 1 \Rightarrow \lim_{x \to 0} \frac{f(x)}{g(x)} = 1 \Rightarrow \lim_{x \to 0} \frac{1 - e^{-x}}{x} = 1 \quad //$$

Visual Evidence of Theorem:

Graphs of $y = x$ & $y = 1-e^{-x}$

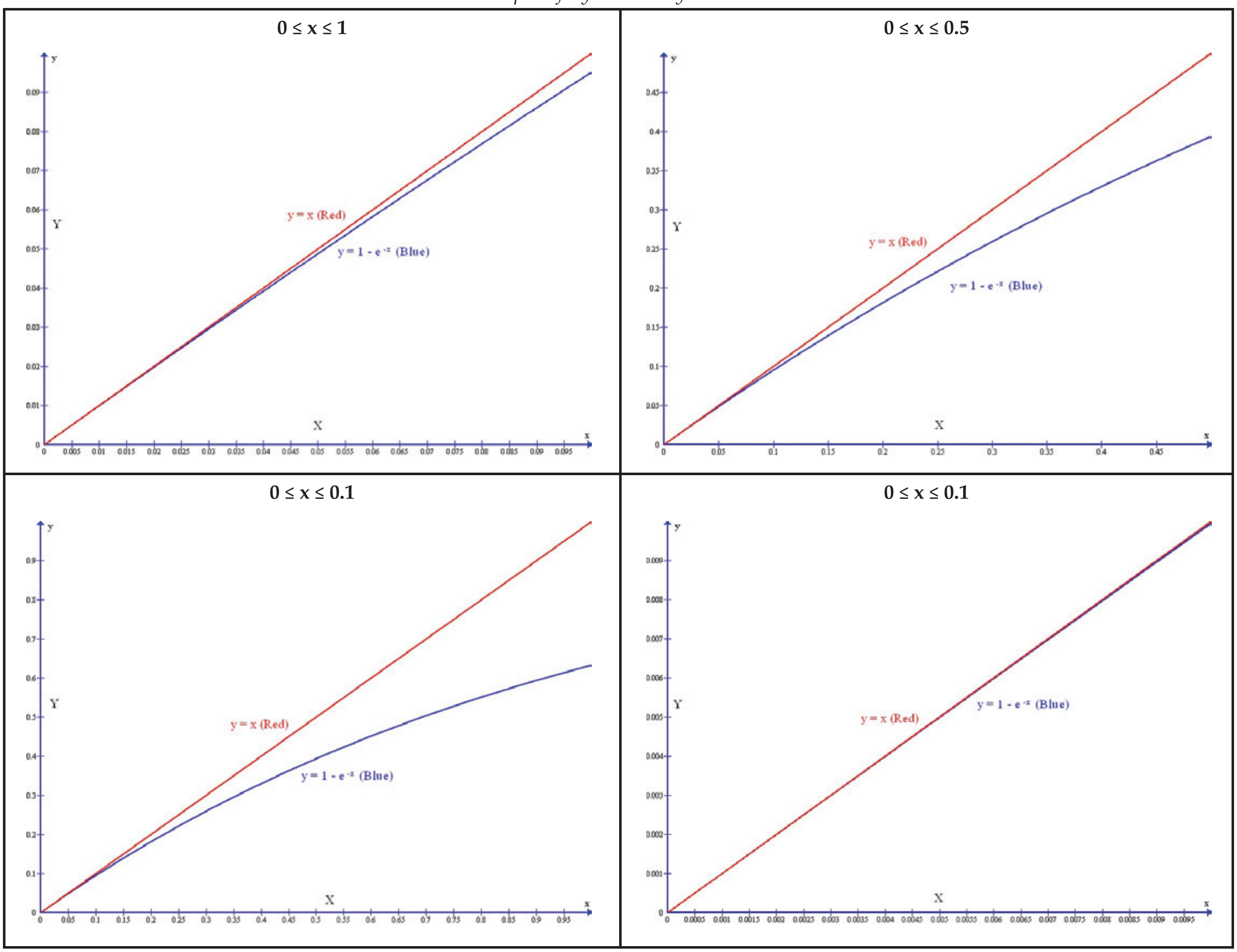

Note: as x gets closer to zero how the blue and red graphs become super-imposed.

Please fax completed survey to
315.351.4209 – ATTN: Journal Editor

RIAC JOURNAL SURVEY

SECOND QUARTER - 2010

Journal Format ☐ Hard Copy ☑ Web Download

How satisfied are you with the **content** (article technical quality) in *this issue* of the Journal?

☐ Very Satisfied ☐ Satisfied ☐ Neutral ☐ Dissatisfied ☐ Very Dissatisfied

How satisfied are you with the **appearance** (layout, readability) of *this issue* of the Journal?

☐ Very Satisfied ☐ Satisfied ☐ Neutral ☐ Dissatisfied ☐ Very Dissatisfied

How satisfied are you with the **overall quality** of *this issue* of the Journal (compared to similar magazines, newsletters, etc.)?

☐ Very Satisfied ☐ Satisfied ☐ Neutral ☐ Dissatisfied ☐ Very Dissatisfied

How did you become **aware** of *this issue* of the Journal?

☐ Subscribe ☐ Colleague ☐ Library ☐ RIAC Website ☐ RIAC Email ☐ Conference/Trade Show

Would you **recommend** the RIAC Journal to a colleague?

☐ Definitely ☐ Probably ☐ Not Sure ☐ Probably Not ☐ Definitely Not

Please suggest general **changes / improvements** to the RIAC Journal that would improve your level of satisfaction:

____

____

____

____

Please suggest further **topics** for the RIAC Journal that might help it to better meet your needs:

____

____

Overall satisfaction

☐ Very Satisfied (5) ☐ Satisfied (4) ☐ Neutral (3) ☐ Dissatisfied (2) ☐ Very Dissatisfied (1)

CONTACT INFORMATION (OPTIONAL)

Name ____________________ Position/Title ____________________

Organization ____________________ Office Symbol ____________________

Address ____________________ City __________ State __________ Zip __________

Country ____________________ Email ____________________

Phone ____________________ Fax ____________________

My Organization is: ☐ Army ☐ Navy ☐ Air Force ☐ Other DoD/Government ☐ Industry ☐ Academic ☐ Other

I need help with a reliability, maintainability, quality, supportability, or interoperability problem. ☐ Please contact me

Reliability Information Analysis Center
100 Seymour Road | Suite C101 | Utica, NY 13502-1348

THE RIAC ONLINE

- The RIAC's "Desk Reference" is a Virtual Knowledge Base of reliability know-how on best practices, analyses and test approaches.
- Save time and money at the RIAC's online store where you can browse, order, and immediately download electronic versions of most of the RIAC's products.

- Online Product Store
- RMQSI Library
- Technical Answers
- The RIAC Journal
- Upcoming Training Courses
- What's New at RIAC